



*Non-abelian Quantum Hall States on the
Thin Torus*

Emma Wikberg

Licentiate thesis in theoretical physics

Akademisk avhandling för avläggande av
licentiatexamen i teoretisk fysik vid
Stockholms universitet

Department of Physics
Stockholm University

April 2009

Abstract

We explore various quantum Hall systems on a torus. As the torus circumference L_1 becomes small, hopping terms in the interacting hamiltonian diminish and the problem is greatly simplified.

Earlier studies of the gapless system of fermions at Landau level filling $\nu = 1/2$ showed that within a range of L_1 on the very thin torus, the low-energy sector may be mapped onto 1D spin-1/2 chains. In this regime, the resulting spin hamiltonian is dominated by the nearest neighbor spin flip. This is the known XY-model, which is exactly solvable in terms of neutral dipoles with gapless excitations. The solution has high overlap with the Rezayi-Read wave function that describes this system.

The same mapping is here applied to $\nu = 5/2$, half-filling in the second Landau level, which as opposed to $\nu = 1/2$ is a gapped quantum Hall system well described by the non-abelian Moore-Read (MR) wave function. In this case the spin hamiltonian is dominated by a ferromagnetic next-nearest neighbor Ising term, yielding sixfold degenerate ground states, in agreement with what is known about the MR wave function. We also find the expected gapped fractionally charged excitations to appear as domain walls between different ground states.

Mathematically, there is a connection between fermions in a quantum Hall system and bosons in rapidly rotating Bose-Einstein condensates. Here, bosons at $\nu = 1$ is the analog to fermions at half-filling. Led by this we find a way to map the bosonic system onto a spin-1/2 space, in analogy to the mapping for fermions above. As for $\nu = 5/2$ we find the spin hamiltonian to be dominated by the negative next-nearest neighbor Ising interaction, which in this case yields a threefold degeneracy of the ground states. Furthermore, gapped fractionally charged excitations emerge as domain walls between the ground states. Again, this agrees well with what is expected from the non-abelian Moore-Read wave function that describes the $\nu = 1$ phase.

In addition to the above we explore a pseudopotential connection between $\nu = 1/2$ and $\nu = 5/2$, giving an idea of the stability of these phases.

Exact diagonalization studies and overlap calculations support the theoretical conclusions drawn.

Furthermore, we expand the picture of fractional charges as domain walls to more general (bosonic and fermionic) filling fractions, and sketch a way to count the excitation degeneracies.

Acknowledgements

I wish to express my gratitude to my supervisor Anders Karlhede, for being patient and helpful, and for sharing his wide knowledge and sense for a good research project.

A big thank you to Emil, who has been supportive and helpful in every possible way throughout my work.

I also want to acknowledge everyone else who has contributed to the appended papers; Eddy, Hans and Janik.

And finally thank you to my friends (formerly or presently) at Fysikum for very good company and discussions.

Contents

List of accompanying papers	4
1 Introduction and outline	5
1.1 Introduction	5
1.2 Outline	7
2 The Hall experiments	8
2.1 The classical Hall effect	8
2.2 The quantum Hall effect	8
2.3 Basic theory	11
2.3.1 Fractional charges and statistics	13
3 The one-dimensional model	16
3.1 Electron in a magnetic field	16
3.2 A lattice model	19
3.2.1 Fock space representation and symmetries	19
3.2.2 Field operator hamiltonian	24
3.3 The thin limit	26
3.3.1 What happens with the interaction terms	26
3.3.2 Fractional charges in the thin limit	27
3.3.3 Connection to the bulk	28
4 Exploring half-filled Landau levels on the thin torus	30
4.1 Fermions at $\nu = 1/2$	30
4.1.1 Spin model, exact solution	31
4.2 Fermions at $\nu = 5/2$	35
4.2.1 Same spin model, other coefficients...	36
4.3 Pseudopotential investigation	39
4.3.1 The pseudopotential method	39
4.3.2 Results	41

5	Spin chain description of bosons at $\nu = 1$	47
5.1	How bosons enter the quantum Hall effect	47
5.1.1	Connection between bosons and fermions at different fillings	48
5.2	Mapping of $\nu = 1$ onto 1D spin-1/2 chain	49
5.2.1	The subspace and mapping rules	49
5.2.2	Spin operator hamiltonian	51
6	More on non-abelian quantum Hall states	57
6.1	Ground states and elementary excitations on the thin torus . .	57
6.1.1	Ground states	57
6.1.2	Excitations	58
6.1.3	Connection to CFT	61
7	Conclusions and outlook	62
	Appendix	64

List of accompanying papers

- Paper I **Pfaffian quantum Hall state made simple: multiple vacua and domain walls on a thin torus**
E.J. Bergholtz, J. Kailasvuori, E. Wikberg, T.H. Hansson,
and A. Karlhede
Phys. Rev. B **74** 081308(R) (2006), [arXiv:cond-mat/0604251]
- Paper II **Degeneracy of non-abelian quantum Hall states on the torus: domain walls and conformal field theory**
E. Ardonne, E.J. Bergholtz, J. Kailasvuori, and E. Wikberg
J. Stat. Mech. (2008) P04016, [arXiv:0802.0675]
- Paper III **Spin chain description of rotating bosons at $\nu = 1$**
E. Wikberg, E. J. Bergholtz, and A. Karlhede
Preprint, [arXiv:0903.4093]

Chapter 1

Introduction and outline

1.1 Introduction

The integer quantum Hall effect (IQHE) was discovered in 1980 by von Klitzing¹, Dorda and Pepper [1]. Two years later, the even more interesting fractional quantum Hall effect (FQHE) was discovered by Tsui, Störmer and Gossard [2]. Since then it has been the object of interest for many research projects, but still the FQHE offers challenging mysteries not yet resolved.

The quantum Hall effect (QHE) arises in two-dimensional electron gases exposed to strong magnetic fields perpendicular to the surface. Classically, there is a linear relation between the Hall resistance in the sample and the strength of the magnetic field, B . However, as the temperature gets low, the magnetic field grows large and the samples get cleaner, the resistance gets quantized. When the resistance is plotted as a function of B , plateaus emerge at the values $R_{xy} = \frac{h/e^2}{\nu}$. ν here is a fractional number and is called the filling fraction. The emergence of the plateaus is a nontrivial consequence of the interaction between the electrons.

In spite of the relatively simple experimental setup, the theory behind the FQHE contains several peculiar phenomena like e.g. fractional charge and statistics [3]. Behind some of the greatest theoretical achievements stand Laughlin [4] and Jain [5], who have e.g. constructed microscopical wave functions describing several quantum Hall systems². These commonly accepted theories describing the quantum Hall system are very successful, but not everything is based on a complete microscopical understanding of the problem.

Earlier work [6, 7] has lead to interesting results on generic filling frac-

¹von Klitzing was awarded the Nobel Prize five years later for his achievement.

²Laughlin shared a Nobel Prize with Tsui and Störmer.

tions in the lowest Landau level when the system is put on a thin torus. In particular, a microscopical exact solution for the low-energy sector of $\nu = 1/2$ has been found. There the system is mapped onto a spin-1/2 chain, and a truncated spin hamiltonian reveals the gapless nature of this (non-QH) state. Encouraged by this we here expand this analysis to include fermions at filling $\nu = 5/2$.

The 'pfaffian' Moore-Read state [8], which is believed to describe the $\nu = 5/2$ system, exposes several interesting and unusual features. For example, fractional charges $\pm e/4$ appear as excitations of the degenerate ground states. The fractionally charged excitations, called non-abelian anyons, obey non-abelian statistics, that qualitatively differs from the statistics of fermions, bosons and abelian anyons. This property has led to an interesting discussion of whether the $\nu = 5/2$ system can be used in future quantum computing, and as such this is a subject within quantum physics that receives great attention.

In spin language the clear difference in nature between $\nu = 1/2$ and $\nu = 5/2$ may be explained by the fact that different spin interactions dominate the hamiltonian. For filling $\nu = 1/2$ a nearest neighbor spin flip is the most important term, leading to a ground state of free neutral dipoles (with small corrections it becomes a Luttinger liquid [9]). At $\nu = 5/2$ on the other hand, a next-nearest neighbor Ising term competes with the hopping. A bold truncation of the hamiltonian suggests sixfold degenerate ground states with gapped fractionally charged excitations, in good agreement with what is known about the Moore-Read wave function.

For approximately a decade the mathematical equivalence between fermions in a quantum Hall system and rapidly rotating Bose-Einstein condensates (BEC) has been known [10, 11]. For example, one believes that bosons at filling $\nu = 1$ display properties very similar to fermions at $\nu = 5/2$ (fractional charges, non-abelian statistics etc.). This motivates a study of the bosonic system on the thin torus. A spin-1/2 description here suggests a microscopic understanding analogous to $\nu = 5/2$, with a dominating next-nearest neighbor Ising term. In this case it leads to a threefold degeneracy of the ground state, and fractional charges $\pm e/2$, in agreement with the bosonic Moore-Read wave function [8].

It is worth mentioning that rotating BEC:s perhaps will be even better candidates for construction of decoherence free quantum qubits than the fermionic quantum Hall system [12]. If one would be able to realize the lowest Landau level physics in a BEC, it would possibly be easier to control in the laboratory. Therefore it seems particularly exciting to explore $\nu = 1$ on the thin torus.

1.2 Outline

In chapter 2 we give a short introduction to the classical as well as the quantum Hall effects. We also present a brief review of some of the basic theories behind the QHE and introduce the concepts of fractional charges and fractional statistics.

In chapter 3 we consider electrons in a magnetic field on a cylinder. First we treat the non-interacting case and derive the single-particle wave functions and introduce the concept of Landau levels. This is then used to construct a one-dimensional lattice model, where each single-particle state is either occupied or empty, of the interacting two-dimensional many-particle system in a single Landau level. This mapping of the 2D quantum Hall system to a 1D lattice model is exact in the strong magnetic field limit. We generalize this to the geometry of a torus and construct a field operator hamiltonian. We also give a rather comprehensive discussion of the various symmetries of the model. At the end of the chapter we discuss the thin limit of the model, i.e. when the circumference of the torus goes to zero.

A major part of this thesis focuses on a spin-1/2 description of three different systems—gapless fermions at filling fraction $\nu = 1/2$, gapped fermions at $\nu = 5/2$ and gapped bosons at $\nu = 1$. In chapter 4 we treat the two half-filled fermionic systems by first reviewing an elegant solution of $\nu = 1/2$ in terms of spin on the thin torus. This is then expanded and applied to half-filling in the second Landau level, shining light on the very different properties of the two systems. We also explore a connection between the two by means of pseudopotentials. The analysis treats both ground states and fractionally charged excitations. See also paper I ([13]) and III ([14]), both attached to this thesis.

In chapter 5 we introduce the mapping of bosons at $\nu = 1$ onto 1D spin-1/2 chains. In analogy with the above we present a truncated spin hamiltonian which we believe gives new insight in why this system realizes a gapped Moore-Read phase. We find the correct degenerate ground states as well as fractionally charged excitations, which like for fermions emerge as domain walls between different ground states. See also paper III.

The ground state degeneracy and excitations as domain walls between these may be generalized to a large class of (bosonic and fermionic) filling fractions. The principles for this are treated in chapter 6, where we also mention a connection between the counting of quasiparticle/quasihole degeneracies and combinatorics as well as conformal field theory. The details concerning this chapter can be found in paper II ([15]).

The last chapter summarizes the results presented in the thesis and presents an outlook towards further research possibilities.

Chapter 2

The Hall experiments

2.1 The classical Hall effect

The Hall effect arises when a conducting plate is placed in a magnetic field \mathbf{B} perpendicular to the surface, and a current \mathbf{I} is driven through the plate (see Fig. 2.1). With the coordinate axes chosen as in the figure, $\mathbf{B} = B\hat{z}$ and $\mathbf{I} = I\hat{x}$.

If one considers the classical picture of this system, each electron is affected by the Lorentz force $\mathbf{F} = q\mathbf{v} \times \mathbf{B}$, where the charge $q = -e = -|e|$. Since the velocity \mathbf{v} at equilibrium is antiparallel to the current and perpendicular to the magnetic field, the electrons will experience a force pointing in the negative y -direction. As the charged particles accumulate at one side of the metal plate, a potential difference builds up. In equilibrium the magnetic force will balance the electric repulsion between the electrons, and an easy calculation shows that the potential difference V_y becomes proportional to B . In 1879, the American physicist Edwin Hall [16] discovered this linear behavior when he plotted the so-called Hall resistance $R_{xy} = V_y/I$ against the magnitude of the magnetic field—the result was, as we now expect, a straight line. This simple phenomenon is called the (classical) Hall effect.

2.2 The quantum Hall effect

About a century after Hall's achievement, in 1980, the quantum version of the Hall effect was discovered by Klaus von Klitzing and co-workers [1]¹. At very low temperature and in strong magnetic fields, electrons in interfaces between semi-conductors form a two-dimensional electron gas (i.e., they are unable

¹An introduction to the physics of the quantum Hall effect is found in [17].

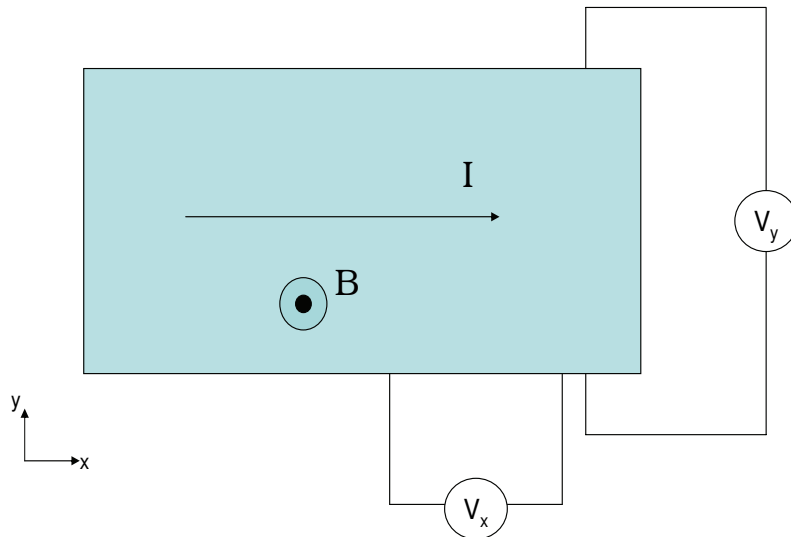


Figure 2.1: *The setup for the Hall experiment.*

to move in the z -direction). Under these conditions, and if the sample has a small (but crucial) amount of disorder, the previously linear dependence of B is destroyed. Instead, a quantization of the Hall resistance appears. von Klitzing observed that when the magnetic field strength varies, the Hall resistance $R_{xy} = V_y/I$ jumps between plateaus of specific values (see Fig. 2.2), namely

$$R_{xy} = \frac{R_K}{n}, \quad n = 1, 2, 3, \dots, \quad (2.1)$$

where $R_K = h/e^2$ is the so called von Klitzing constant. Note also from the figure that, as R_{xy} forms plateaus, the longitudinal resistance $R_{xx} = V_x/I$ drops to zero. Because the denominator n is an integer, this behavior of the system is now called the integer quantum Hall effect. It can be explained by first solving the quantum mechanical problem of an electron in a magnetic field (see section 3.1).

2.3 Basic theory

As mentioned earlier, the IQHE can be understood by investigating the quantum mechanical properties of a single electron in a magnetic field. It turns out that the degenerate energy levels of such an electron are those of a harmonic oscillator, i.e.

$$E_n = (n + 1/2)\hbar\omega_c, \quad n = 0, 1, \dots, \quad (2.3)$$

where $\omega_c \equiv \frac{eB}{mc}$ is the cyclotron frequency. These energy levels are called Landau levels, after the Russian physicist L.D. Landau (1908-1968) [19] who was the first to solve this problem. In the low temperature limit (i.e. the quantum Hall regime), the electrons in the two-dimensional electron gas will simply occupy the states with the lowest energies, if electron-electron interaction is ignored. Each Landau level has a degeneracy that depends on the strength of the magnetic field. The number of states N_S within each energy level is

$$N_S = \frac{BA}{\Phi_0}, \quad (2.4)$$

where A is the area of the Hall plate and Φ_0 is the magnetic flux quantum, $\Phi_0 = \frac{hc}{e}$. In other words, N_S is given by the number of flux quanta penetrating the system. We may now define a very important quantity, namely the filling fraction ν ;

$$\nu = \frac{N_e}{N_S} = \frac{N_e\Phi_0}{BA}, \quad (2.5)$$

where N_e is the number of electrons in the sample. If we let the electrons fill the lowest available single-particle states, ν will be the number of filled Landau levels. The ν that appears in equation (2.2) is closely related to the filling fraction. The plateau with $R_{xy} = \frac{R_K}{\nu}$ is namely centered around the value $B = \frac{N_e\Phi_0}{\nu A}$, and we can now comment on the emergence of the IQHE. When ν is an integer, the ν lowest lying Landau levels will be completely filled and there is an energy gap $\hbar\omega_c$ to the next level. In presence of disorder in the system, this energy gap will lead to a plateau in the resistance, i.e. changing the magnetic field around these points will keep R_{xy} constant. The detailed theory explaining this is a bit complicated, and will not be a subject of this thesis. The interested reader can read about Laughlin's so-called gauge argument in [20].

In general, the requirements for the quantum Hall effect to appear, besides low temperature and high magnetic fields, are some finite amount of disorder in the system, and a finite energy gap. Disorder is of course always present in the experimental situation.

The difficulty in understanding the fractional effect lies in the fact that, for fractional fillings, there are many ways of arranging the electrons within the highest occupied Landau level. Without interaction between the electrons this would lead to many degenerate many-particle states (and a gap to the next Landau level, as for the integer effect). However, the interaction lifts this degeneracy and the physics is completely determined by the filling and the inter-particle interaction, as excitations within the Landau level are possible. For some filling fractions there is a gap, whereas some fillings have a continuous energy spectrum. Indeed, for $\nu = 1/2$ and some other fractions, the resistance is not quantized (i.e. no gap!), but there are many examples of fractional fillings which display plateaus in the resistance curve, as seen in Fig. 2.2. Clearly the interaction between the electrons, which could be neglected when considering the IQHE, plays a crucial role in the FQHE and render a gap that will give rise to a quantization of R_{xy} . At these fillings the many-body ground state must have a gap in energy to the excited states.

Consequently, it is a great challenge to understand the physics at various fractional fillings ν . Several attempts have been made to solve these mysteries. Laughlin's wave functions for $\nu = \frac{1}{2m+1}$ [4] are very important. This construction was generalized to all fillings p/q , q odd, in [21, 22]. An alternative (but equivalent) picture of the specific fractions $\nu = \frac{p}{2pm+1}$ was given by Jain [5, 23, 24]. Here, both m and p are integers, which gives odd denominator fillings.

In the plane, the Laughlin wave function reads

$$\Psi_{\frac{1}{2m+1}}(z_1, z_2, \dots, z_{N_e}) = \prod_{i<j} (z_i - z_j)^{2m+1} e^{-\frac{1}{4} \sum_i |z_i|^2}, \quad (2.6)$$

where $z = x + iy$ and (x, y) are the particle coordinates in the plane. The numbers 1 to N_e label the electrons. Note that the polynomial factor leads to an antisymmetric wave function (fermions!) and that it makes the total function rapidly shrink to zero for electrons close to each-other. This trial wave function is an extremely good approximation to the ground state at $\nu = \frac{1}{2m+1}$, and it predicts both the expected gap and excitations with fractional charge $\pm \frac{e}{2m+1}$.

Jain's wave function is a good approximation for $\nu = \frac{p}{2mp+1}$ and reads

$$\Psi_{\frac{p}{2mp+1}}(z_1, z_2, \dots, z_{N_e}) = \mathcal{P}_{LLL} \prod_{i<j} (z_i - z_j)^{2m} \Psi_p, \quad (2.7)$$

where Ψ_p is the state with the p lowest Landau levels completely filled and \mathcal{P}_{LLL} projects the entire state on the lowest Landau level. Jain also introduced so-called composite fermions to explain the FQHE. Composite

fermions are electrons 'bound to' an even number of flux quanta, which so-to-say reduces the magnetic field and thus increases the filling fraction (see Fig. 2.3). More specifically, the 'new' magnetic field becomes

$$B^* = B - 2m\nu B. \quad (2.8)$$

In that way, Jain proposes, one can interpret the FQHE at e.g. $\nu = 1/3$ as a system of composite fermions at $\nu = 1$. In other words, we may see it as the IQHE but with a new kind of particles. Another element of this construction is that the composite fermions are non-interacting.

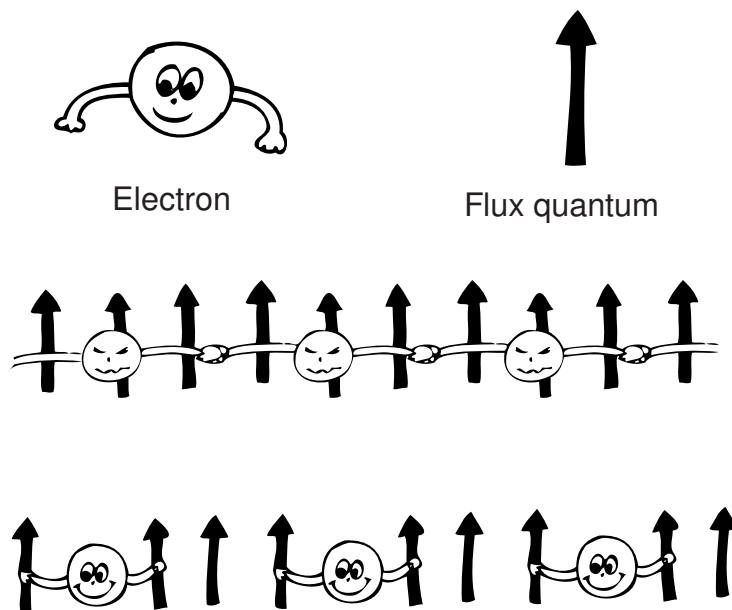


Figure 2.3: *An illustration of the composite fermion construction at $\nu = 1/3$. The strongly interacting electrons are seen as free composite fermions in a reduced magnetic field. The idea of the caricature is taken from Kwon Park.*

The strength of the composite fermions is that they describe the system at different filling fractions to a very high accuracy, but they have also been criticized for not providing a good microscopical understanding (see e.g. [25]) and basic questions remain to be answered.

2.3.1 Fractional charges and statistics

The FQHE is a topic that contains many unusual phenomena. In this thesis we will among other things treat the appearance of fractional charges. Just

as it sounds, it means that there are excitations that behave like particles with fractions of an electron charge. In general, the gapped Jain states at $\nu = \frac{p}{2mp+1}$ have excitations with fractional charges $\pm \frac{e}{2mp+1}$. This will be further discussed in section 3.3.2.

Even more exotic phenomena are fractional and non-abelian statistics, which differ from the statistics of bosons and fermions. Let us consider two indistinguishable particles, and think about what must happen if we let one of the particles go around the other particle and then return to its initial position. We require the operation to be adiabatic, i.e. we require finite gaps between the energy levels and move the particle so slowly that there is no energy transferred to the system. Suppose that the system initially is in the ground state. The adiabatic process then assures that the system is not excited to some higher energy level during the operation.

In three dimensions, there is no unambiguous definition of encircling a specific point in space, and the path can be contracted into a point. But this is the same thing as if nothing has happened and thus this operation must return the same state. Furthermore, it yields the same result as letting the two particles switch positions twice. Just interchanging the two particles clearly corresponds to half of the operation above, and should thus return the initial state with a factor of either plus or minus one in front. Fermionic (bosonic) statistics means that, because we are dealing with indistinguishable particles which can not (can) be in the same state, we must get a minus (plus) sign in front of the wave function when we let the two particles interchange. In other words, the wave function is antisymmetric (symmetric).

More possibilities appear when we consider the same operation in two dimensions. In that case there is really a way of defining what it means to go around a specific point. We may not shrink the path to a point, and can thus not say that nothing has happened. Clearly, if there is no degeneracy of the ground state, we must return to the same physical state after the operation. There is however a possibility of the original state being multiplied by a phase factor. Half of the operation, i.e. interchanging the two particles then also yields a phase factor $e^{i\phi}$. This kind of statistics is called fractional statistics [3]. The particles obeying this are called anyons and appear as quasiparticles in the Laughlin and Jain states. It is possible, but not yet established, that this behavior was observed experimentally in 2005 [26].

A generalization of fractional statistics is non-abelian statistics, which means that interchanging two particles (so-called braiding) yields an entirely new state. This phenomenon appears when there is a degeneracy of the states. Since there is no energy transfer needed to put the system in the degenerate state, the adiabatic process does not prevent the particles from switching to the other states. Non-abelian and fractional statistics are very

hot research subjects, both because of their exotic properties and, in the former case, since it could possibly play an important role in future quantum computing [27].

Chapter 3

The one-dimensional model

In this chapter we solve the quantum mechanical problem of a single electron on a cylinder with a magnetic field perpendicular to its surface. We use this to find an expression for the many-particle hamiltonian on the cylinder and then on a torus. This leads to a mapping of the two-dimensional system onto a one-dimensional lattice. We also show how letting the circumference of the torus go to zero provides a nice way to study the quantum Hall system, and argue that many features of the large system remain in that thin limit.

3.1 Electron in a magnetic field

Since the quantum Hall effect takes place in a magnetic field perpendicular to a two-dimensional electron layer, a reasonable thing to do is to calculate the energy eigenstates for one of these electrons. We do this using the geometry of a cylinder and then generalize our results to the electron gas on a torus.

We want to study the situation in Fig. 3.1, where L_1 is the circumference of the cylinder. We are free to choose a gauge, and the so-called Landau gauge,

$$\mathbf{A} = By\hat{x}, \quad (3.1)$$

gives us a magnetic field pointing in the negative z -direction since $\mathbf{B} = \nabla \times \mathbf{A} = -B\hat{z}$.

As usual, we may start with the hamiltonian of a free particle in two dimensions and modify this by minimal coupling:

$$\mathbf{p} \rightarrow \mathbf{p} - \frac{q}{c}\mathbf{A}, \quad (3.2)$$

which yields

$$H = \frac{1}{2m} \left(\left(p_x + \frac{eB}{c}y \right)^2 + p_y^2 \right). \quad (3.3)$$

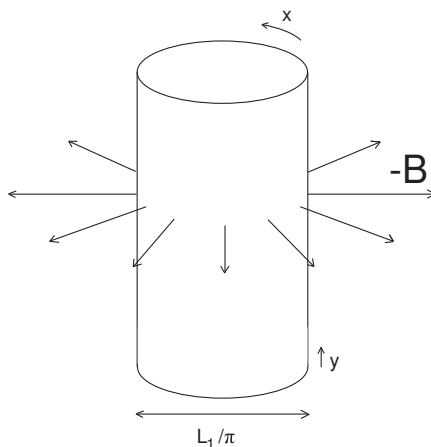


Figure 3.1: An illustration of a cylinder with a magnetic field \mathbf{B} perpendicular to the surface.

The question is: What are the energy eigenfunctions of this hamiltonian?

A good choice of separating ansatz is

$$\psi_k(x, y) = e^{ikx} \phi(y). \quad (3.4)$$

Also, we should have periodic boundary conditions in the x -direction, i.e.

$$\psi_k(x, y) = \psi_k(x + L_1, y), \quad (3.5)$$

which implies

$$k = \frac{2\pi q}{L_1}, \quad q = 0, \pm 1, \dots \quad (3.6)$$

The wave function (3.4) is clearly an eigenstate of p_x with the eigenvalue $\hbar k$. This means that we are allowed to replace the p_x operator by $\hbar k$ in the hamiltonian, and the x -dependance is eliminated. We can then divide both sides in the Schrödinger equation by e^{ikx} , and we are left with

$$H_k \phi(y) = E_k \phi(y), \quad (3.7)$$

with

$$H_k \equiv \frac{1}{2m} (p_y^2 + (\hbar k + \frac{eB}{c} y)^2). \quad (3.8)$$

We recognize this as the hamiltonian of a one-dimensional harmonic oscillator, and can immediately write down the energy eigenvalues:

$$E_{nk} = (n + 1/2) \hbar \omega_c, \quad n = 0, 1, \dots, \quad (3.9)$$

where $\omega_c \equiv \frac{eB}{mc}$ is the cyclotron frequency. As mentioned in chapter 2.1, these energy levels are called Landau levels.

Note also that, according to eq. (3.8), the wave functions are centered around $y = -k\ell^2$, where $\ell \equiv \sqrt{\frac{\hbar c}{eB}}$ is the so-called magnetic length. With this definition, the energy eigenfunctions become

$$\psi_{nk}(x, y) = \frac{1}{\sqrt{\pi^{1/2} 2^n n! L_1}} e^{ikx} H_n(y + k\ell^2) e^{-\frac{1}{2\ell^2}(y+k\ell^2)^2}, \quad (3.10)$$

where H_n are the Hermite polynomials with $H_0 = 1$, $H_1(\xi) = 2\xi$, $H_2(\xi) = 4\xi^2 - 2$ etc..

Since the difference between two consecutive k -values is $\frac{2\pi}{L_1}$, the distance between the centers of the associated wave functions is $\frac{2\pi\ell^2}{L_1}$, as illustrated by Fig. 3.2. In the following section this will be used to form a lattice model for the quantum Hall system, but first we would like to again identify the filling fraction ν . The area per state in a Landau level is $2\pi\ell^2$ (see Fig. 3.2), so the density of states is $n_s = 1/2\pi\ell^2$. If we let n_e be the electron density, the number of filled Landau levels is

$$\nu = \frac{n_e}{n_s} = 2\pi\ell^2 n_e = \frac{\hbar c n_e}{eB} = \frac{n_e \Phi_0}{B}, \quad (3.11)$$

which agrees with equation (2.5).

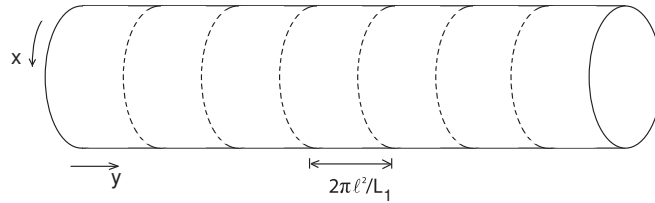


Figure 3.2: *The single particle states are centered along lines passing through the points $y = -k\ell^2$, a distance $2\pi\ell^2/L_1$ apart.*

Through the rest of this work we let $\ell = 1$, i.e. the area per state is 2π . With L_2 being the length (in the y -direction) of the cylinder, this leads to the relation $L_1 L_2 = 2\pi N_s$.

3.2 A lattice model

We now turn to considering the full quantum Hall problem, i.e. the interacting many-particle system. We restrict our studies to the lowest Landau level ($n = 0$), assuming that the electrons will occupy only the states with the lowest energies¹. This presumption will be true in the limit $B \rightarrow \infty$, where the gap between the Landau levels grows large. That all electrons are in the lowest Landau level means that they have the same kinetic energy. The sum of these energies is a constant that can be subtracted from the hamiltonian, which we may then regard as consisting of the potential of the electron-electron interaction only². Finally, we assume that we have complete spin-polarization—the large magnetic field will force all the electrons to have the same spin.

3.2.1 Fock space representation and symmetries

With these approximations we may consider many-particle states where each single-particle state $\psi_k(x, y)$ is either occupied by an electron or empty³. The single-particle states are centered along lines (see Fig. 3.2) that one can picture as sites in a one-dimensional lattice. Hence, we can perform a mapping onto a series of zeros and ones (Fock space representation), where a one at the k :th position denotes an electron in the state centered at $y = -k$ in units of the lattice spacing $2\pi/L_1$ (see Fig. 3.3)⁴. In other words, a one at this position corresponds to an electron with x -momentum $-\frac{2\pi}{L_1}k$ and k is here an integer. The correspondence between states in the lattice model and the single-particle states is, since we are dealing with fermions, a Slater determinant⁵:

$$|n_0 \ n_1 \dots \ n_{N_s-1}\rangle \doteq \frac{1}{\sqrt{N_e!}} \begin{vmatrix} \psi_{k_1}(\mathbf{r}_1) & \psi_{k_1}(\mathbf{r}_2) & \dots & \psi_{k_1}(\mathbf{r}_{N_e}) \\ \psi_{k_2}(\mathbf{r}_1) & \psi_{k_2}(\mathbf{r}_2) & \dots & \psi_{k_2}(\mathbf{r}_{N_e}) \\ \vdots & \vdots & \ddots & \vdots \\ \psi_{k_{N_e}}(\mathbf{r}_1) & \psi_{k_{N_e}}(\mathbf{r}_2) & \dots & \psi_{k_{N_e}}(\mathbf{r}_{N_e}) \end{vmatrix}, \quad (3.12)$$

¹Later we will also consider $\nu = 5/2$, which is in the second Landau level. However, we will treat even this case as belonging to the lowest level, but with modified electron-electron interaction.

²Interaction with the disorder in the system is ignored.

³Here, $\psi_k(x, y) = \psi_{0k}(x, y)$, i.e. the wave functions of the lowest Landau level. We could also have chosen to consider the system in e.g. the second Landau level, in which case we would have $\psi_k(x, y) = \psi_{1k}(x, y)$.

⁴The first lattice site to the left here corresponds to $k = 0$.

⁵Below, \doteq means that the state is *represented* by the wave function in position space of the particles, i.e. $|n\rangle \doteq \psi(\mathbf{r})$ means $\langle \mathbf{r}|n\rangle = \psi(\mathbf{r})$ etc.

where $n_i = 0, 1$ and $\sum_{i=0}^{N_s-1} n_i = N_e$. N_s is as before the number of states in the Landau level. A general many-particle state with N_e electrons is then constructed as a superposition of these states.

To make this clear, let us look at a system of just two electrons at filling $\nu = 1/2$. Suppose that one of them has zero momentum and one of them has a momentum corresponding to $k = 3$. The total wave function is then

$$\begin{aligned} |1001\rangle &\doteq \frac{1}{\sqrt{2}} \begin{vmatrix} \psi_0(\mathbf{r}_1) & \psi_0(\mathbf{r}_2) \\ \psi_3(\mathbf{r}_1) & \psi_3(\mathbf{r}_2) \end{vmatrix} = \\ &= \frac{1}{\sqrt{2}} [\psi_0(\mathbf{r}_1)\psi_3(\mathbf{r}_2) - \psi_0(\mathbf{r}_2)\psi_3(\mathbf{r}_1)]. \end{aligned} \quad (3.13)$$

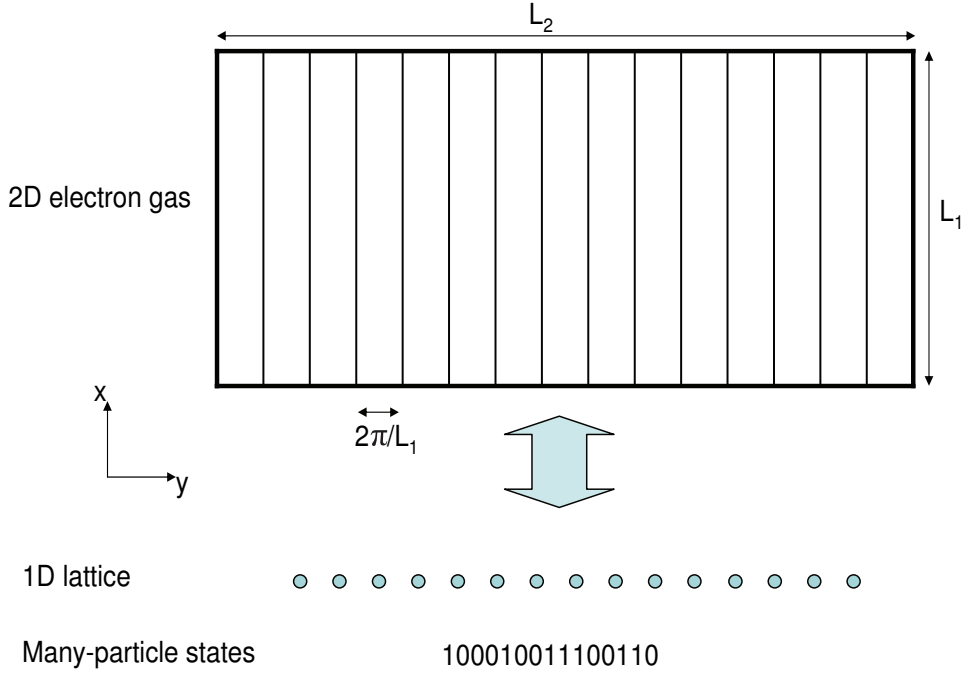


Figure 3.3: An illustration of the mapping between the single-particle states centered around different positions in a one-dimensional lattice. The many-particle basis states can be written as series of zeros and ones—the illustration shows one example of this.

Following Haldane [28], we will now introduce two translation operators, T_1 and T_2 , that act on the many-particle states described above. Consider a torus, i.e. our cylinder but with the ends connected so that the first and last sites are separated by one lattice constant. Hence we may require periodic

boundary conditions also in the y -direction. We define T_2 to be an operator that translates the entire lattice configuration one step to the right (i.e. in the positive y -direction);

$$T_2|n_0 n_1 \dots n_{N_s-1}\rangle = |n_{N_s-1} n_0 \dots n_{N_s-2}\rangle. \quad (3.14)$$

T_1 is a translation operator acting in the x -direction, basically it picks out the x -momenta of the electrons, and the eigenvalues are $e^{\frac{i2\pi}{N_s} \sum_{k=0}^{N_s-1} kn_k} \equiv e^{i2\pi K/N_s}$. The lattice states of eq. (3.12) are eigenstates of T_1 ;

$$T_1|n_0 n_1 \dots n_{N_s-1}\rangle = e^{i2\pi K/N_s}|n_0 n_1 \dots n_{N_s-1}\rangle, \quad (3.15)$$

where

$$K = \sum_{k=0}^{N_s-1} kn_k \text{ mod } N_s. \quad (3.16)$$

K is thus the sum of the momenta (in units of $2\pi/L_1$) of the particles in the lattice, taken modulo N_s . This quantum number characterizes the eigenstates of T_1 . In the two-particle state described above, $K = 0 + 3 = 3$.

Because of the translation invariance on the torus, both T_1 and T_2 commute with the hamiltonian in one Landau level, i.e. $[T_1, H] = [T_2, H] = 0$. However, $[T_1, T_2] \neq 0$. But let us now consider the electron gas at filling $\nu = p/q = N_e/N_s \Leftrightarrow pN_s = qN_e$. What happens if we let T_2^q act on one of the lattice states (which are eigenstates of T_1)? Each electron will move q steps to the right, increasing K with $N_e q$. Some of them, though, might at the same time 'fall over the edge' of the lattice, appearing at the left end again (remember the torus symmetry!). This will decrease K by mN_s , where m is the number of electrons falling over the edge. Summarizing, acting with T_2^q on an eigenstate of T_1 gives a change in K that is $\Delta K = N_e q - mN_s = (p - m)N_s$. Because p and m are integers, taking $\Delta K \text{ mod } N_s$ gives zero. This means that the operator T_2^q conserves the quantum number of T_1 and hence that $[T_2^q, T_1] = 0$. Since $[T_2, H] = 0$ it also follows that $[T_2^q, H] = 0$.

The operators T_1 and T_2^q form a maximal set of commuting operators together with the hamiltonian, H . The three operators are simultaneously diagonalizable, and their common eigenstates constitute a complete basis set. This fact makes the procedure of diagonalizing the hamiltonian easier and faster if we let the wanted energy eigenstates be eigenstates of T_1 and T_2^q as well. H will conserve the quantum numbers of T_1 and T_2^q , and so the matrix representation of H in this basis will only have non-zero elements for coupling between eigenstates with the same quantum numbers.

Since acting with T_2 on a state with N_s lattice sites N_s times must give back the original state, we have $T_2^{N_s} = 1$, i.e. the eigenvalue of $T_2^{N_s}$ is 1. We are interested in the eigenvalues of T_2^q . We rewrite $1 = T_2^{N_s} = (T_2^q)^{N_s/q}$, which implies that the eigenvalues of T_2^q are $a_N = e^{i2\pi Nq/N_s}$, where $N = 0, 1, \dots, \frac{N_s}{q} - 1$. N is thus the quantum number of T_2^q .

Let us now construct the eigenstates of T_2^q . Since we also search for eigenstates of T_1 , we require that each state in these combinations have the same K -value. This will however cause no trouble if we follow the following procedure. For each eigenvalue a_N , start with one of the states $|n_0 n_1 \dots n_{N_s-1}\rangle \equiv |\tilde{\Psi}\rangle$ and form the (unnormalized) state

$$|\Psi\rangle \equiv (1 + a_N^{-1}T_2^q + a_N^{-2}T_2^{2q} + \dots + a_N^{-(N_s/q-1)}T_2^{q(N_s/q-1)})|\tilde{\Psi}\rangle. \quad (3.17)$$

One can easily show that these states will be eigenstates of T_2^q , i.e. $T_2^q|\Psi\rangle = a_N|\Psi\rangle$. For some choices of a_N and $|\tilde{\Psi}\rangle$, the expression in (3.17) will however give a trivial zero, in which case we have tried to match the eigenvalue with the wrong state. This method can clearly be used for any $\nu = p/q$ and N_s .

Here it is appropriate to comment on the degeneracy of the energy eigenstates. Since H and T_2 commute, it follows that translation between 1 and $q-1$ steps in the y -direction of a state yields new states with the same energy:

$$\begin{aligned} H|\Psi\rangle &= E|\Psi\rangle \Rightarrow \\ HT_2|\Psi\rangle &= ET_2|\Psi\rangle, \\ HT_2^2|\Psi\rangle &= ET_2^2|\Psi\rangle, \\ &\vdots \\ HT_2^{q-1}|\Psi\rangle &= ET_2^{q-1}|\Psi\rangle. \end{aligned} \quad (3.18)$$

Acting once more with T_2 on $|\Psi\rangle$ will return the first equation, since $|\Psi\rangle$ is an eigenstate of T_2^q as well. Note that all these translated states have different K -values, hence they are orthogonal. Thus we have shown that there is a q -fold degeneracy of the many-particle energies at filling $\nu = p/q$. This was first pointed out by Haldane [28].

Example

In this thesis, we first study the case $\nu = 1/2$, in which each state is labeled by the quantum numbers K and N of T_1 and T_2^2 respectively. One task is thus to find the combinations of different states $|n_0 n_1 \dots n_{N_s-1}\rangle$ that are eigenstates of T_1 and T_2^2 . Since we search for eigenstates of T_1 , we require that each state in these combinations have the same K -value; thus, for example, $|1100\rangle + |1010\rangle$ is not allowed since $|1100\rangle$ has $K = 1$ and $|1010\rangle$ has $K = 2$.

Again, let us look at the simple example of two electrons at four sites. First note that the number of ways to arrange two identical particles at four different sites is $\binom{4}{2} = 6$. We list the different possibilities and their K -values here:

$$\begin{aligned} &|1100\rangle; K = 1, \\ &|1010\rangle; K = 2, \\ &|1001\rangle; K = 3, \\ &|0110\rangle; K = 3, \\ &|0101\rangle; K = 4 \text{ mod } 4 = 0, \\ &|0011\rangle; K = 5 \text{ mod } 4 = 1. \end{aligned}$$

The second state above is the only one with $K = 2$, hence it can not be connected to any of the other states. We note that it is the eigenstate of T_2^2 with quantum number $N = 0$, since $T_2^2|1010\rangle = |1010\rangle = e^{i2\pi 0/2}|1010\rangle$. A similar thing holds for the fifth state, which has $K = 0$ and $N = 0$.

What about the four remaining states? Two by two they share the same K -value, but neither of them is alone an eigenstate of T_2^2 . If we do not immediately see the solution, we may use the general method described above. Let us for example try with $a_N = a_1 = -1$ and $|\tilde{\Psi}\rangle = |1001\rangle$:

$$|\Psi\rangle = \left(1 + \frac{1}{-1}T_2^2\right)|\tilde{\Psi}\rangle = |1001\rangle - |0110\rangle \quad (3.19)$$

so that

$$T_2^2|\Psi\rangle = |0110\rangle - |1001\rangle = -|\Psi\rangle = a_1|\Psi\rangle. \quad (3.20)$$

Thus, $|1001\rangle - |0110\rangle$ has $(K, N) = (3, 1)$, and so on. This and the rest of the results are summarized below:

$$\begin{aligned} &|1010\rangle; (K, N) = (2, 0), \\ &|0101\rangle; (K, N) = (0, 0), \\ &|1100\rangle + |0011\rangle; (K, N) = (1, 0), \\ &|1100\rangle - |0011\rangle; (K, N) = (1, 1), \end{aligned}$$

$$\begin{aligned} &|1001\rangle + |0110\rangle; (K, N) = (3, 0), \\ &|1001\rangle - |0110\rangle; (K, N) = (3, 1). \end{aligned}$$

For $\nu = 1/2$, the degeneracy of the energy eigenvalues is 2, and the degenerate states are translations one step in the y -direction of each-other. We check this by noting that e.g. $|1010\rangle$ and $|0101\rangle$ are related by this kind of translation. Also, it is evident from eq. (3.18) that they have the same energy.

3.2.2 Field operator hamiltonian

The just described lattice model provides a simple way to construct the hamiltonian for the electron-electron interactions, and (at least in the thin limit, as will be clear in the next section) explore the eigenstates of that operator.

Let us define the field operator $\hat{\Psi}^\dagger(\mathbf{r})$:

$$\hat{\Psi}^\dagger(\mathbf{r}) \equiv \sum_k \psi_k^*(\mathbf{r}) c_k^\dagger, \quad \{c_n^\dagger, c_m\} = \delta_{mn}, \quad (3.21)$$

where c_k^\dagger (c_k) is an operator that creates (destroys) an electron in the state ψ_k . One can then write the electron density as $\hat{\rho}(\mathbf{r}) = \hat{\Psi}^\dagger(\mathbf{r})\hat{\Psi}(\mathbf{r})$ and the hamiltonian for the interaction energy between the electrons is⁶

$$\begin{aligned} H &= \frac{1}{2} \int \int : \hat{\rho}(\mathbf{r}_1) V(\mathbf{r}_1 - \mathbf{r}_2) \hat{\rho}(\mathbf{r}_2) : d^2 r_1 d^2 r_2 = \\ &= \sum_{k_1 k_2 k_3 k_4} V_{k_1 k_2 k_3 k_4} c_{k_1}^\dagger c_{k_2}^\dagger c_{k_3} c_{k_4} \end{aligned} \quad (3.22)$$

where the matrix elements are

$$V_{k_1 k_2 k_3 k_4} = \frac{1}{2} \int \int \psi_{k_1}^*(\mathbf{r}_1) \psi_{k_2}^*(\mathbf{r}_2) V(\mathbf{r}_1 - \mathbf{r}_2) \psi_{k_3}(\mathbf{r}_2) \psi_{k_4}(\mathbf{r}_1) d^2 r_1 d^2 r_2. \quad (3.23)$$

The symbol $::$ means that the product of operators is normal ordered, i.e. all creation operators are put to the left of the annihilation operators (this is a way of preventing the empty lattice from yielding non-zero energy terms).

Here we just state that on the torus one finds that [29]

$$V_{k_1 k_2 k_3 k_4} = \frac{\delta'_{k_1+k_2, k_3+k_4}}{2N_s} \sum_{q_1, q_2} \delta'_{k_1-k_4, q_1} \tilde{V}(\mathbf{q}) e^{-\frac{q^2}{2} - i(k_1-k_3)\frac{q_2 L_2}{N_s}}, \quad (3.24)$$

⁶Compare with the classical expression $H_{cl} = \frac{1}{2} \int \int \rho(\mathbf{r}_1) V(\mathbf{r}_1 - \mathbf{r}_2) \rho(\mathbf{r}_2) d^2 r_1 d^2 r_2$.

where $\tilde{V}(\mathbf{q})$ is the two-dimensional Fourier transform of $V(\mathbf{r})$ and δ' is the periodic Kronecker delta (with period N_s). The sum is taken over all allowed wave vectors on the torus, i.e. $q_\alpha = \frac{2\pi n_\alpha}{L_\alpha}$, $n_\alpha = 0, \pm 1, \dots$. For Coulomb, the Fourier transform of $V(\mathbf{r}) = \frac{1}{r}$ is $\tilde{V}(\mathbf{q}) = \frac{1}{q}$.

The sum in eq. (3.22) contains two kinds of electrostatic terms. For $k_1 = k_4$, $k_2 = k_3$ particle 1 and 2 keep their original k -values (compare with eq. (3.23))—this is called the direct interaction. There is also the possibility for $k_1 = k_3$, $k_2 = k_4$, which corresponds to particle 1 and 2 switching places in the lattice—this is referred to as the exchange interaction. Remember that the electrons are indistinguishable, so that the hop does not change the state. We will therefore refer to these terms as electrostatic. The hamiltonian also contains so-called hopping terms, where the above conditions for k_i are not fulfilled. For both cases however, the total momentum of the particles must be conserved—or, the position of the center of mass must be preserved. Since the different sites are numbered with the momenta of the states, we have the condition $k_1 + k_2 = k_3 + k_4$, which readily eliminates one of the sums in (3.22).

In the case of the geometry of a torus, we have periodic boundary conditions in the y -direction as well. Translating all the electrons the same number of lattice sites should not change the energy of the system. This leads to an extra requirement on k_i , i.e. we need only two indices on the V factor, and the hamiltonian for the torus can be written

$$\begin{aligned} H &= \sum_i \sum_{|m| < k \leq N_s/2} V_{km} c_{i-k}^\dagger c_{i+m}^\dagger c_{i-k+m} c_i = \\ &= \sum_i \sum_{0 \leq m < k \leq N_s/2} V_{km} c_{i-k}^\dagger c_{i+m}^\dagger c_{i-k+m} c_i + h.c. \equiv \sum_{0 \leq m < k \leq N_s/2} \hat{V}_{km}, \end{aligned} \quad (3.25)$$

where

$$\begin{aligned} V_{km} &= \frac{1}{2^{\delta_{k, N_s/2}}} (V_{i+m, i+k, i+m+k, i} - V_{i+m, i+k, i, i+m+k} \\ &\quad + V_{i+k, i+m, i, i+m+k} - V_{i+k, i+m, i+m+k, i}). \end{aligned} \quad (3.26)$$

It is evident from eq. (3.25) that V_{k0} is the electrostatic interaction energy between two electrons at the distance k from each-other. V_{km} ($m \neq 0$) gives the energy of the hopping of two electrons at the distance $k+m$ to a distance of $k-m$, as illustrated by Fig. 3.4.

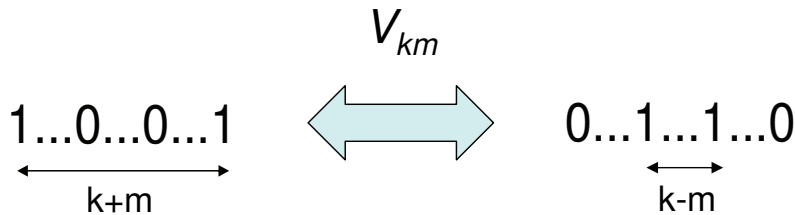


Figure 3.4: V_{km} is the matrix element for hopping between the two states above. Note that the hopping preserves the total momentum (or, equivalently, the position of the center of mass).

3.3 The thin limit

The idea of describing the quantum Hall system on a torus is of course a mathematical construction. When we let the circumferences in both the x - and the y -directions go to infinity, we will recover the real experimental planar geometry. It thus sounds a bit strange at first, wanting to explore the model in the opposite limit, i.e. letting $L_1 \rightarrow 0$. Surprisingly though, it has earlier been shown [7] that many of the physical features of the quantum Hall system survive in this limit. Moreover, the theoretical calculations and considerations become much simpler, therefore this limit should be profitable to explore. The reason for the simplification is the fact that, as $L_1 \rightarrow 0$, all hopping terms in the hamiltonian vanish. The ground state (and other energy eigenstates) of the remaining electrostatic terms will just be certain 'crystalline' configurations where the electrons are located in specific patterns that minimize the electrostatic repulsion.

3.3.1 What happens with the interaction terms

It can be seen from equation (3.23) that hopping becomes unimportant as $L_1 \rightarrow 0$. As we already know, in this limit the lattice sites become widely separate. This means that the overlap between two wave functions centered at different lattice points tends to zero. For hopping terms, the wave functions for four different k -values are multiplied to give the matrix elements, thus they become extremely small. For the electrostatic exchange terms, the matrix elements are

$$V_{k_1 k_2 k_3 k_4} = \frac{1}{2} \int \int \psi_{k_1}^*(\mathbf{r}_1) \psi_{k_2}^*(\mathbf{r}_2) V(\mathbf{r}_1 - \mathbf{r}_2) \psi_{k_1}(\mathbf{r}_2) \psi_{k_2}(\mathbf{r}_1) d^2 r_1 d^2 r_2. \quad (3.27)$$

We see that only two different wave functions are involved. However, $\psi_{k_1}^*$, ψ_{k_1} and $\psi_{k_2}^*$, ψ_{k_2} are evaluated in different points in space, and hence even

these overlaps will be extremely small. In contrast, the direct terms are

$$V_{k_1 k_2 k_3 k_4} = \frac{1}{2} \int \int \psi_{k_1}^*(\mathbf{r}_1) \psi_{k_2}^*(\mathbf{r}_2) V(\mathbf{r}_1 - \mathbf{r}_2) \psi_{k_2}(\mathbf{r}_2) \psi_{k_1}(\mathbf{r}_1) d^2 r_1 d^2 r_2, \quad (3.28)$$

in which case we get non-zero overlaps even though ψ_{k_1} , ψ_{k_2} are widely separated.

We conclude that, in the thin limit, all interaction terms except for the direct electrostatic V_{k_0} are suppressed. The possibility to neglect all hopping and exchange terms of course simplifies many calculations. Specifically, the ground states of the repulsive two-body electrostatic interaction are the crystalline states where all particles are as far separated as possible. For example, at filling $\nu = 1/q$ this implies one particle on every q :th site. In general, these thin limit ground states are called Tao-Thouless (TT) states [30].

3.3.2 Fractional charges in the thin limit

In section 2.3.1 we mentioned the exotic phenomenon of fractional charges in the quantum Hall system. We will now take advantage of the crystalline-like states in the thin limit to explore how fractional charges can be created in a lattice state [31, 32]. We will argue that an electron/hole added to the $\nu = 1/q$ system gives rise to fractional charges $\pm e/q$. The procedure below is called the Su-Schrieffer counting argument [33].

As an example, consider a lattice state at $\nu = 1/3$. In the thin limit we may consider the TT ground state

$$|\dots 100100100100100100100100100100\dots\rangle.$$

Now, what happens if we erase three holes at well separated positions, and at the same time add one unit cell 100 somewhere else⁷? The lattice state becomes

$$|\dots 100\underline{101}00100100\underline{101}00100100\underline{101}00100\dots\rangle.$$

At the three places where we erased a hole, there are concentrations of negative charge (red color and underlined in the sequence). But compared to the original lattice state above, there is only one more electron in total in the series. Therefore, we must see the three charge collections as sharing this extra charge $-e$. We conclude that each hole deleted from the $\nu = 1/3$ system has

⁷In this way we can compare systems of the same size.

given rise to a fractional charge $-e/3$. Obviously, the opposite thing holds for *adding* holes, in which case they contribute with a charge $+e/3$ compared to the original system. Note also that because the above example resulted in one extra electron charge, adding an electron to the $\nu = 1/3$ system yields three $-e/3$ charges. Adding one electron and one hole yields a ground state containing two $-e/3$ charges, and so on.

In general, adding one hole (i.e. a flux quantum) to the $\nu = 1/q$ system yields a contribution of charge $+e/q$. These fractional charges are actually the $L_1 \rightarrow 0$ limits of the quasiholes that appear in the bulk near the Laughlin fractions $\nu = \frac{1}{2m+1} = \frac{1}{q}$ for odd q . A construction similar to the above can be made to find the fractional charges of the Jain states at $\nu = \frac{p}{2mp+1}$, which are $\pm \frac{e}{2mp+1}$ [7]. Fractional charges appear in excitations of the ground states at the exact fillings. Here, one positive and one negative fractional charge of the same size appear at different places in the lattice states. Due to the opposite signs, the quasiparticles attract each-other and the more separate they are the larger energy has the excited state. However, when moving slightly away from the exact filling (e.g. adding or removing an empty site from $\nu = 1/3$), the fractional charges appear in the ground state.

The half-filled system is of particular interest to us. At $\nu = 1/2$, fractional charges appear only in the thin limit. For the state $|101010\dots\rangle$, adding an electron (without changing the number of sites) gives rise to two fractional charges $-e/2$, and adding a hole (one empty site) gives one charge $+e/2$. Adding one electron and one site yields one $-e/2$ charge. These formations are the crystalline ground states at and near half-filling in the thin limit. The bulk state $\nu = 1/2$ is gapless and fractional charges do not appear in that case. However, at $\nu = 5/2$, half-filling in the second Landau level, an interesting thing happens due to an additional nontrivial degeneracy of the ground state. Adding an electron plus one site (one empty site) will, even in the bulk, lead to a ground state where the fractional charge $-e/2$ ($+e/2$) has divided into two charges of magnitude $e/4$. The formation of these fractional charges in the thin limit will be discussed further in section 4.2.

The appearance and counting of fractional charges will be generalized in chapter 6, when we treat the Read-Rezayi states at filling $\nu = \frac{k}{kM+2}$ on the thin torus.

3.3.3 Connection to the bulk

In recent studies of the QH system on the torus [7, 34, 35], the connection between the thin torus and the bulk has been explored. Good arguments have been given for that the crystal ground states at $\nu = \frac{p}{q}$, q odd, in the thin limit evolve continuously to the abelian quantum Hall states in the bulk.

This implies that the TT ground states of these fractions, in spite of their simplicity, display the important physics of the bulk; the gap, the correct quantum numbers and the fractionally charged excitations.

For fillings with no gap (e.g. $\nu = 1/2$), and non-abelian QH fillings (e.g. $\nu = 5/2$ and bosons at $\nu = 1$) on the other hand, there must be a phase transition between the two. However, this phase transition takes place on a very thin torus and the physics can still be understood by studying the physics on a thin (but not infinitely thin) torus. We will see several examples of this in the following chapters.

The many-particle wave functions, like Laughlin's in (2.6), given in this thesis are all expressed in the planar geometry. On the torus they depend on the circumference, and it is thus possible to study them as L_1 approaches zero. This gives us ground states etc. that may be compared with our analytical conjectures as well as numerical results. Comments on this will appear several times in this thesis.

Chapter 4

Exploring half-filled Landau levels on the thin torus

In this chapter we will use our knowledge about the thin torus to investigate two very different systems on a similar basis. Our starting point will be a previously known spin description of the gapless fermions at filling $\nu = 1/2$, which we will expand and compare with half-filling in the second Landau level, $\nu = 5/2$. We will also use a so-called pseudopotential expansion to investigate a connection between the two phases.

4.1 Fermions at $\nu = 1/2$

As previously hinted at, the fractional fillings without gaps (the metallic states) are as complicated to understand as the gapped ones. The absence of a gap is not only a consequence of the filling, but also of the electron-electron interaction. Hence, it is nontrivial to describe the metallic states. A successful wave function for the gapless $\nu = \frac{1}{2m}$ ground state was constructed by Rezayi and Read [36] and looks like¹

$$\Psi_{\frac{1}{2m}}(z_1, z_2, \dots, z_N) = \mathcal{P}_{LLL} \det[e^{i\mathbf{k}_i \cdot \mathbf{r}_j}] \prod_{i < j} (z_i - z_j)^{2m} \prod_i e^{-\frac{1}{4}|z_i|^2} \quad (4.1)$$

on the plane. Remember the composite fermions from section 2.3 and the reduced magnetic field in eq. (2.8). With $\nu = 1/2$, $m = 1$, we get $B^* = B - B = 0$. We can thus picture this system as the non-interacting composite fermions moving in zero magnetic field—free composite fermions! From this

¹Another model, a mean field theory, for these systems has been developed by Halperin, Lee and Read [37].

perspective the Slater determinant of plane waves in (4.1) is logical. \mathcal{P}_{LLL} projects the state onto the lowest Landau level.

That $\nu = 1/2$ can be described by free composite fermions nicely explains why the state is gapless. The ground state is constructed by letting the free fermions fill the states with lowest momenta in a Fermi sea. The excitations are then realized by just deforming the Fermi sea—as the size of the system grows large, these excitation energies become extremely small since the Fermi sea becomes more dense.

4.1.1 Spin model, exact solution

Another microscopical explanation for the absence of a gap was given by Bergholtz and Karlhede [6, 7]. They studied $\nu = 1/2$ on the thin torus, in a regime where the low-energy sector may be mapped onto a 1D spin-1/2 chain. The ground state in this regime is described by an exact solution of a truncated hamiltonian on a thin but finite torus. The state gives a description of the half-filled system in terms of neutral dipoles in one dimension. Since the net charge of these quasiparticles is zero, there is no coupling to the magnetic field. Moreover, the particles are nearly free and the system is gapless. This is reminiscent of the composite fermion construction, where one gets non-interacting particles in a reduced (zero) magnetic field. We will here review the basic and most important features of this study, and later we expand the analysis to fermions at filling $\nu = 5/2$ and bosons at $\nu = 1$.

Consider $\nu = 1/2$ on the torus. In the thin limit, $L_1 \rightarrow 0$, the ground state is the TT state $|101010\dots\rangle$ (and the trivial translation $|010101\dots\rangle$). Like all TT states it is gapped and thus differs from the gapless bulk state. We will now investigate what happens when we increase the circumference from zero and hopping terms start to compete with the electrostatics.

Assume that we are in a regime where the electrostatic repulsion between the particles still plays a major role, such that the low energy sector is built up of states where each pair of sites $2i, 2i + 1$ contains exactly one particle and one empty site (a copy of this restricted Hilbert space is obtained for the pairs $2i - 1, 2i$). Every such pair can then be assigned a spin according to

$$10 \rightarrow \uparrow, \quad 01 \rightarrow \downarrow. \quad (4.2)$$

In this way, the many-particle states in this subspace, which we call \mathcal{H}'_f , are mapped onto a spin-1/2 chain. The mapping is obviously reversible.

Not all hopping terms in the hamiltonian (3.25) preserve \mathcal{H}'_f . This means that in all energy states we will have more or less mixing of states inside and outside the subspace. However, processes involving the shortest range hop-

ping \hat{V}_{21} , which is the dominant hopping term on the thin torus, always preserves the subspace. Because of this (and the strong electrostatic repulsion), we assume that the low energy states only have negligible contributions from states outside of \mathcal{H}'_f . We may then discard all hopping processes that take us out of the subspace. Under this condition, all terms in the hamiltonian can (for acting *only within the subspace*) be translated into spin operators, and one finds the truncated hamiltonian

$$\hat{H}'_f = \sum_i \sum_{k=1}^{N_s/2} \left[\frac{\alpha_k}{2} (s_i^+ s_{i+k}^- + h.c.) + \beta_k s_i^z s_{i+k}^z \right] \quad (4.3)$$

where

$$\alpha_k = 2V_{2k,1}, \quad (4.4)$$

$$\beta_k = 2V_{2k,0} - (1 - \delta_{k,N_s/4})V_{2k+1,0} - V_{2k-1,0}. \quad (4.5)$$

To be explicit, the spin flips correspond to hopping and the Ising terms correspond to electrostatics. Specifically, the shortest hopping equals the nearest neighbor spin flip;

$$\hat{V}_{21} = V_{21} \sum_i (s_i^+ s_{i+1}^- + h.c.) = \frac{\alpha_1}{2} \sum_i (s_i^+ s_{i+1}^- + h.c.). \quad (4.6)$$

This rewriting in terms of spin operators acting within \mathcal{H}'_f is advantageous since we have gone from a quartic hamiltonian (3.25) to a quadratic, which is simpler to analyze.

The next step towards understanding would be to investigate the values of the coefficients α_k and β_k , and we will do this as a function of the torus circumference L_1 . In Figure 4.1 we have plotted the largest coefficients between $L_1 = 4$ and $L_1 = 8$ for Coulomb and a short-range interaction ($\nabla^2\delta$). We see that as L_1 decreases, the hopping terms α_1, α_2 tend to zero as expected, and the hamiltonian is dominated by the electrostatic repulsion. In this thin limit regime the TT state is the lowest in energy. However, as we go to the right in the diagram we see how the shortest hopping coefficient α_1 grows in comparison to the β -terms, and from $L_1 \sim 5$ it is actually the dominant one. This is not obvious for Coulomb interaction (right panel). However, there is strong numerical evidence that the system realizes the same phase as for the short-range interaction, and from $L_1 \sim 5$ up to $L_1 \sim 8$ it is a valid approximation to truncate the hamiltonian (4.3) further to

$$\hat{H}'_f \approx \frac{\alpha_1}{2} \sum_i (s_i^+ s_{i+1}^- + h.c.). \quad (4.7)$$

This hamiltonian describes the so-called XY-spin chain. It is exactly solvable in terms of free neutral fermions (dipoles), and the system is as such gapless. The ground state is homogeneous, consisting of the very "hoppable" (with \hat{V}_{21}) state $|11001100\dots\rangle = |\uparrow\downarrow\uparrow\downarrow\dots\rangle$ and all kinds of spin flips on this. Of course, since we are making an approximation, this will never be the exact ground state of the full hamiltonian. However, as long as other terms are sufficiently small, we will remain in a gapless phase more generally called a Luttinger liquid [9].

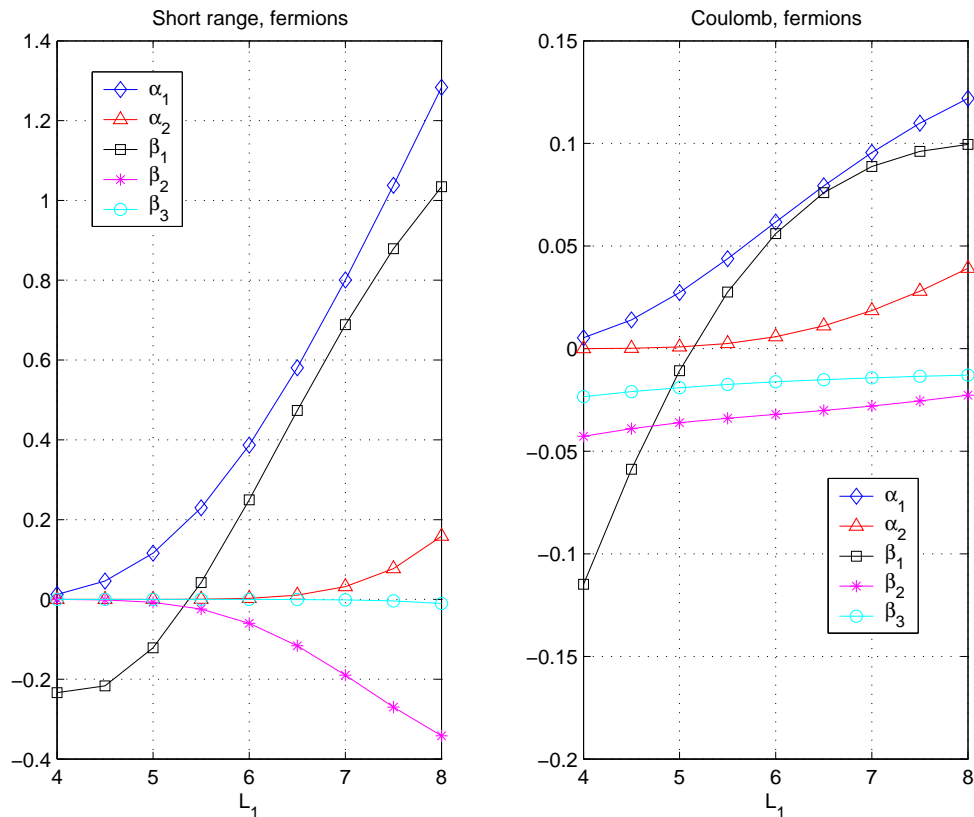


Figure 4.1: Here we show the values of the leading coefficients in the spin-chain hamiltonian for fermions with different interactions, $V(\mathbf{r})$. The leftmost figure corresponds to a short-range interaction, $V(\mathbf{r}) = \nabla^2\delta_p(\mathbf{r})$, and to the right we have Coulomb interaction. The plot is constructed for $N_s = 16$, but changing the system size does not change the curves significantly.

Let us now compare this analysis with what one actually gets when per-

forming exact diagonalization on $\nu = 1/2$ [7]². A simplified phase diagram for Coulomb interaction is presented in Figure 4.2. For very thin tori, the ground state at $\nu = 1/2$ is the crystal $|1010\dots\rangle$. At $L_1 \approx 5.3$, however, there is a first order phase transition to a homogeneous state (the XY- or Luttinger phase), with contributions from the hoppable $|1100\dots\rangle$. The state has large overlap with the ground state of the hamiltonian (4.7). It has also large overlap with the Rezayi-Read wave function, and it evolves continuously to the bulk system as $L_1 \rightarrow \infty$.

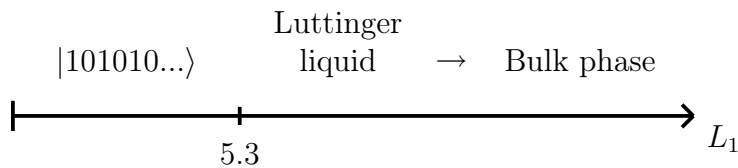


Figure 4.2: The phase diagram of fermions at $\nu = 1/2$ and Coulomb interaction as a function of L_1 . The diagram looks approximately the same for particle number from 4 at least up to 9.

Of course, as L_1 becomes so large that other hopping terms than \hat{V}_{21} become important, the truncation in equation (4.7), and hence the exact solution, is no longer valid (this happens at around $L_1 = 8$ for up to nine particles). However, there are indications that the physics remains qualitatively the same, and evidence has been found that for gapless and non-abelian QH states in general, the infinitely thin torus and the bulk are separated by exactly one phase transition, whereas for abelian QH states, the ground state of the infinitely thin torus evolves continuously to the bulk state³. However, in both cases the thin torus contains much of the physics of the experimental system. In the light of the above we will now make an attempt to find a similar description of half-filling in the second Landau level.

²The input to the computer program is the number of particles, N_e , and sites, N_s , the circumference L_1 and the potential. The program computes the matrix elements of the hamiltonian in the basis of the T_1 and T_2^q eigenstates and diagonalizes the matrix. This gives which superpositions of these eigenstates that are also eigenstates of H , and their energies. Each energy eigenstate is thus labeled by the energy and the quantum numbers K and N . Due to limited computer capacity we have been restricted to systems of up to ten particles. In particular we have focused on the case of $N_e = 8$.

³The latter follows from the analytical and numerical studies of the Laughlin wave function for $\nu = 1/3$ on the thin cylinder by Rezayi and Haldane [38], as pointed out in [6]; See also Seidel et al [39].

4.2 Fermions at $\nu = 5/2$

Fermions at $\nu = 5/2$, i.e. the second Landau level being half-filled, is one of the gapped QH systems. In 1991, Moore and Read [8] wrote down a many-particle wave function that is believed to describe this system well. The function, which is also called the pfaffian wave function, is a construction that describes the $\nu = 5/2$ system as being in the lowest Landau level. The completely filled energy level (lowest Landau level with both spin up and spin down) has all electrons in fixed states and they form a uniform background as seen by the other electrons. Hence they do not affect the interaction properties and may be disregarded. The Moore-Read wave function on the plane reads

$$\Psi_{\text{Pf}}(\{z_i\}) = \text{Pf} \left(\frac{1}{z_i - z_j} \right) \prod_{i < j} (z_i - z_j)^2 e^{-\frac{1}{4} \sum_i |z_i|^2}. \quad (4.8)$$

Note that this function is a product of the bosonic (symmetric) Laughlin wave function (lowest Landau level!) and an antisymmetric 'pfaffian', $\text{Pf} \left(\frac{1}{z_i - z_j} \right)$, which makes the state fermionic. $\text{Pf} \left(\frac{1}{z_i - z_j} \right)$ is the square root of the determinant $\det \left(\frac{1}{z_i - z_j} \right)$, with all diagonal elements equal to zero. For example, for four particles it becomes $\text{Pf} \left(\frac{1}{z_i - z_j} \right) = \frac{1}{(z_1 - z_2)(z_3 - z_4)} - \frac{1}{(z_1 - z_3)(z_2 - z_4)} + \frac{1}{(z_1 - z_4)(z_2 - z_3)}$. The pfaffian wave function is the exact ground state of a repulsive three-body interaction [40, 41] of the form

$$V(\mathbf{r}_i, \mathbf{r}_j, \mathbf{r}_k) = \mathcal{S}_{ijk} \nabla_i^4 \nabla_j^2 \delta^2(\mathbf{r}_i - \mathbf{r}_j) \delta^2(\mathbf{r}_j - \mathbf{r}_k), \quad (4.9)$$

where \mathcal{S}_{ijk} is a symmetrizer and all indices are summed over. This interaction prevents triples of electrons to be close to each-other, and on the thin torus this is manifested in six degenerate ground states of type $|1010\dots\rangle$ and $|1100\dots\rangle$.

In the real physical system however, the electrons are of course interacting not via some strange three-body interaction, but via ordinary (two-body) Coulomb repulsion. In our lattice model we can construct the hamiltonian of this system by calculating the matrix elements V_{km} using the single-particle wave functions in the second Landau level, ψ_{1k} , and the Coulomb interaction. Alternatively, we can describe the same physics⁴ by using the lowest Landau level wave functions ψ_{0k} but with a modified interaction, $V(r)$. For reasons

⁴I.e. obtain the same matrix elements V_{km} . This will yield the same energy spectrum and so on.

that will become clear later, we will mainly choose the latter alternative in this thesis. There are advantages connected to studying the system in the lowest Landau level. One is that the single-particle wave functions⁵ of that level are holomorphic (i.e. analytical) and thus easier to handle.

Despite the similarity of half-filling, the quantum Hall systems at $\nu = 1/2$ and $\nu = 5/2$ are very different. A number of interesting and exotic features of the latter have been found by studying the Moore-Read wave function. It is possible to show that, if the system is studied in the geometry of a torus, the ground state of (4.8) is sixfold degenerate, as compared to the trivial twofold degeneracy expected for fillings $\nu = p/2$. Moreover, if one adds an extra electron to the 5/2-system without changing the number of single-particle states, the extra charge will split into four $-e/4$ charges located at different places. These fractional charges (quasiparticles) obey so-called non-abelian statistics, as mentioned in section 2.3.1 and 3.3.2. We have seen earlier that the creation of fractional charges $\pm e/2$ in the thin limit of $\nu = 1/2$ is a trivial consequence of the crystalline ground states. The appearance of $\pm e/4$ charges at $\nu = 5/2$, on the other hand, is a highly nontrivial phenomenon.

The pfaffian wave function, and the exotic features of the states, have been found using conformal field theory (CFT). This is a field within physics that seemingly has a deep connection to the QHE but the precise reason for this is somewhat obscure. The fact is that the results we get from CFT provides a good description. The study of the $\nu = 5/2$ system on the thin torus sheds light on the degenerate ground states and the origin of the fractional charges.

4.2.1 Same spin model, other coefficients...

Since the lattice model only deals with the highest occupied Landau level, $\nu = 5/2$ is treated in much the same way as $\nu = 1/2$ —half of the lattice sites are occupied and the rest are empty. But the differing interaction in the second Landau level will still lead to other ground states. As mentioned in the previous section, the pfaffian wave function is the exact ground state of a certain three-body interaction. On the thin torus this leads to six degenerate ground states where all triples of particles are as separate as possible, namely those consisting of $|1010\dots\rangle$ (plus one translated state) and $|1100\dots\rangle$ (plus three translations)⁶. As L_1 increases from zero all of them will develop continuously all the way towards the bulk. However, since $\nu = 5/2$ supposedly is a non-abelian QH state, we expect a phase transition to the TT state

⁵This is true if we disregard a trivial gaussian factor common to all states. See eq. (3.10).

⁶When expressed as eigenstates of T_2^2 the latter will come combined, e.g. like $|1100\dots\rangle + |0011\dots\rangle$.

|1010...>) when the torus circumference becomes small enough.

Now, note that all six degenerate ground states above fit into the subspace \mathcal{H}'_f that we defined for $\nu = 1/2$. Hence, on the thin torus they will be well described by the spin hamiltonian (4.3). The values of V_{km} and thus α_k, β_k will however differ from the previous example. Let us compare the respective coefficients by reconstructing the plot in Figure 4.1, this time for Coulomb in the second Landau level. The result is displayed in Figure 4.3.

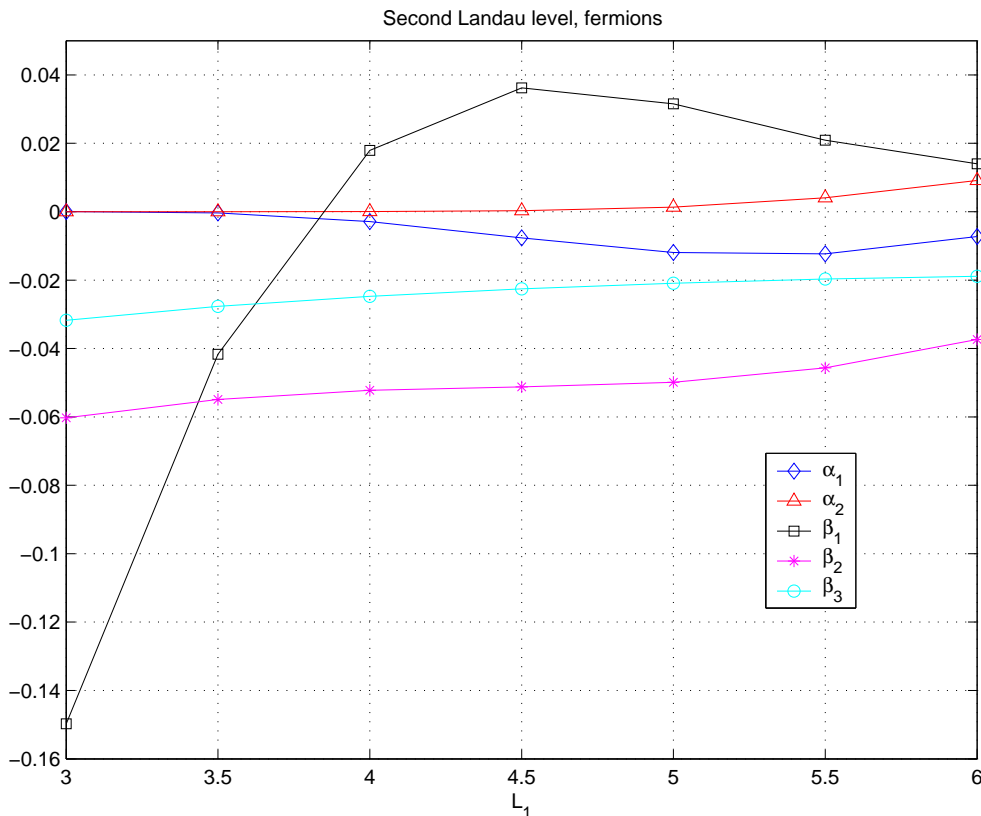


Figure 4.3: Here we show the values of the leading coefficients in the spin-chain hamiltonian for fermions in the second Landau level with Coulomb interaction. The plot is constructed for $N_s = 16$, but changing the system size does not change the curves significantly.

We see that as L_1 goes to zero, the system behaves in the same way as half filling in the lowest Landau level; all hopping terms vanish and we expect the ground state |1010...>). But the graphs differ as we approach the thickness where the nearest neighbor Ising term diminishes compared to the shortest hopping. In this case, when $\beta_1 \approx 0$, the electrostatic coefficient β_2

still remains quite large compared to α_1 . It is interesting to note that if $\beta_2 < 0$ had been the only term in the hamiltonian;

$$\hat{H}'_f \sim \beta_2 \sum_i s_i^z s_{i+2}^z, \quad (4.10)$$

we would have had six exactly degenerate ground states of the types

$$\begin{aligned} |1\rangle &= |\uparrow\uparrow\uparrow\uparrow \cdots\rangle \\ |\tilde{1}\rangle &= |\downarrow\downarrow\downarrow\downarrow \cdots\rangle \\ |2\rangle &= |\downarrow\uparrow\downarrow\uparrow \cdots\rangle \\ |\tilde{2}\rangle &= |\uparrow\downarrow\uparrow\downarrow \cdots\rangle \end{aligned}$$

which exactly correspond to the pfaffian states above, when translated to number representation⁷.

The hamiltonian in (4.10) is minimized by states where all pairs of next nearest neighbors have the same spin. A minimal excitation is created by letting two pairs have opposite spins, which in turn is accomplished by constructing domain walls between the various ground states. Furthermore, these excitations increase the energy of the state by $-\beta_2$ —i.e. we have a gap⁸! Examples of states with minimal excitations are given here:

$$\begin{aligned} &|\uparrow\uparrow\uparrow\uparrow\uparrow\uparrow\uparrow\uparrow\uparrow\uparrow\uparrow\uparrow\downarrow\uparrow\uparrow\uparrow\uparrow\uparrow\uparrow\uparrow\uparrow\uparrow\uparrow\rangle, \\ &|\uparrow\uparrow\uparrow\uparrow\uparrow\uparrow\uparrow\uparrow\uparrow\uparrow\downarrow\uparrow\downarrow\uparrow\uparrow\uparrow\uparrow\uparrow\uparrow\uparrow\uparrow\uparrow\rangle, \\ &|\uparrow\uparrow\uparrow\uparrow\uparrow\uparrow\uparrow\downarrow\uparrow\downarrow\uparrow\downarrow\uparrow\downarrow\uparrow\downarrow\uparrow\uparrow\uparrow\uparrow\uparrow\rangle. \end{aligned}$$

We of course get the same description of excitations as domain walls when we translate the above into number representation. Then it also becomes obvious that the excitations carry fractional charge $\pm\frac{e}{4}$.⁹ Example:

$$|10101\underline{0100}11001100\underline{1101}0101010\rangle,$$

where the blue (red) and underlined is a quasihole (quasiparticle). These fractional charges are also in agreement with one gets from the pfaffian states at $\nu = 5/2$.

One may speculate that the difference in size of the β_2 -term between $\nu = 1/2$ and $\nu = 5/2$ has part in why the latter realizes the pfaffian (and not a gapless Luttinger liquid) phase on the thin torus. In the next chapter we will draw related conclusions when treating bosons at filling $\nu = 1$.

⁷The states $|2\rangle$ and $|\tilde{2}\rangle$ have inequivalent copies in the other choice of subspace while the states $|1\rangle$ and $|\tilde{1}\rangle$ only have equivalent copies—hence, there are six states in total.

⁸In the ground state, all pairs have energy $\beta_2/4$. Here, we have two pairs with opposite spin, each with energy $-\beta_2/4$. Hence the difference in energy compared to the ground state is $-\beta_2$.

⁹See also section 4.3.2.

4.3 Pseudopotential investigation

We have seen both differences and similarities between electrons at half filling in the lowest and second Landau levels. The differences arose because the electron-electron interaction on the basic level is determined by the single-particle wave functions, which in turn depend on the Landau level. In this section we will make a continuous connection between these two systems using so-called pseudopotentials.

4.3.1 The pseudopotential method

The method of studying the quantum Hall system using pseudopotentials was invented by Haldane in the 1980's [42]¹⁰. The idea is to make a kind of Taylor expansion of the potential and vary the expansion parameters. The hamiltonian of any two-body interaction can be written in terms of pseudopotentials as

$$H = \sum_{i < j} \sum_{m=0}^{\infty} V_m P_m(M_{ij}), \quad (4.11)$$

where $P_m(M_{ij})$ projects onto a state where particles i, j have relative angular momentum m and V_m are the pseudopotential parameters, which are real numbers determined by the specific interaction. It can be shown that

$$V_m = \int_0^{\infty} q \tilde{V}(q) L_m(q^2) e^{-q^2} dq, \quad (4.12)$$

where $\tilde{V}(q) = \tilde{H}(q)$ is the Fourier transform of the potential¹¹ and L_m are the Laguerre polynomials; $L_0(q^2) = 1$, $L_1(q^2) = 1 - q^2, \dots$. For Coulomb interaction $\tilde{V}(q) = \frac{1}{q}$, as mentioned in section 3.2.2.

In principle, what one can do is to vary one or several of the pseudopotential parameters, i.e. let $V_m \rightarrow V_m + \delta V_m$, to simulate a new kind of interaction. Varying V_m will yield new matrix elements V_{km} to our hamiltonian, which in turn leads to new energy eigenstates corresponding to the new interaction. In our case, will start from V_{km} as given by the ordinary Coulomb interaction and single-particle wave functions of the lowest Landau level ($\nu = 1/2$), and vary them to yield new states corresponding to Coulomb interaction in the second Landau level ($\nu = 5/2$).

¹⁰Similar ideas have been elaborated by Trugman and Kivelson [43] and by Pokrovsky and Talapov [44].

¹¹Remember that we disregard the kinetic energy since we study only one Landau level.

The logical alternative to this, clearly, would be to keep the Coulomb interaction and just calculate the matrix elements from the single-particle wave functions of the second Landau level (see eq. (3.10) and (3.23)). However, varying the pseudopotential parameters gives an indication of how stable the various phases are, since it allows for continuous change of the interaction. Moreover, it offers the possibility to compare our results with similar studies [41].

As is written in equation (3.26), V_{km} are determined by $V_{k_1 k_2 k_3 k_4}$, which in turn are determined by $\tilde{V}(\mathbf{q})$ as in equation (3.24). We will now vary V_{km} by changing the first pseudoparameter; $V_1 \rightarrow V_1 + \delta V_1$. It can be shown that this is equivalent to letting

$$\tilde{V}(\mathbf{q}) = \frac{1}{q} \rightarrow \frac{1}{q} + 2\delta V_1(1 - q^2). \quad (4.13)$$

The choice to vary V_1 is motivated by the fact this change corresponds to adding a short-range interaction term to the hamiltonian (see below), which is known to be very important in many quantum Hall systems¹². Moreover, the same studies have shown that it is sufficient to vary only δV_1 to find the pfaffian phase.

Connection to real space interaction

We have sketched how to change the interaction terms in the hamiltonian by adding pseudopotential parameters to the Coulomb potential in Fourier space. But how do we relate the change in (4.13) to a real interaction in position space? One can show that the transformed potential $\delta\tilde{V}(\mathbf{q}) = 2\delta V_1(1 - q^2)$ corresponds to a real space interaction of the form

$$\delta V(\mathbf{r}) = 2\delta V_1(1 + \nabla^2)\delta(\mathbf{r}), \quad (4.14)$$

where, again, δV_1 is the pseudopotential parameter we aim to vary.

So what is the physical interpretation of this? Since we are dealing with fermions, the delta function $\delta(\mathbf{r})$ will have no effect on the matrix elements—the electrons can not be at the same position. However, $\nabla^2\delta(\mathbf{r})$ gives rise to a positive potential energy for a pair of particles very close to each-other¹³, so adding a term of this kind to the hamiltonian would favor states where the

¹²The Laughlin wave functions are e.g. exact ground states when only the first expansion terms of (4.11) are non-vanishing.

¹³One can show by partial integration that the expectation value of $\nabla^2\delta(\mathbf{r})$ is nonzero. Although the wave function Ψ must go to zero for $\mathbf{r}_i = \mathbf{r}_j$, there is no such constraint on $\nabla\Psi$.

probability for electrons to come close is small. In contrast, a negative sign in front of $\nabla^2\delta(\mathbf{r})$ would lower the energy of pairs of closely lying electrons relative to the Coulomb case.

The phase we are searching for is the pfaffian ground states of the $5/2$ filling, which we know are exact ground states of a repulsive three-body interaction that separates all triples of particles. On the thin torus they are the crystalline states of type $|10101010\dots\rangle$ and $|11001100\dots\rangle$ (see also chapter 6). Also, $|10101010\dots\rangle$ is the ground state of the ordinary Coulomb interaction at half-filling in the thin limit. But $|11001100\dots\rangle$ is a new state that obviously is favored by a potential that allows for two electrons to be close to each-other. Our guess is therefore that we should choose negative values of δV_1 and thus add a negative $\nabla^2\delta(\mathbf{r})$ to the potential to find the $\nu = 5/2$ phase, starting from $\nu = 1/2$. Note that small values of δV_1 will let the repulsive Coulomb term remain important.

4.3.2 Results

Using the pseudopotential method described in the previous chapter we have investigated the half-filled system on a torus. We have used a computer program for exact numerical diagonalization, where the pseudopotential parameter δV_1 and the length L_1 have been varied to yield different ground states.

A phase diagram for half-filling

As mentioned earlier, most of our computer simulations are done for $N_e = 8$, $N_s = 16$. In Fig. 4.4 we have illustrated the results of these in a phase diagram¹⁴. The ground states of the various potentials and circumferences are separated by lines, and below we give a brief guide to the different phases.

For ordinary Coulomb interaction in the lowest Landau level (i.e. $\delta V_1 = 0$) we find the phases of $\nu = 1/2$. For L_1 up to ~ 5.3 , the ground state is the state evolving from the crystalline state $|1010101010101010\rangle$ ¹⁵. At $L_1 \sim 5.3$ there is a phase transition to the state described by the Luttinger liquid of neutral dipoles, as discussed in section 4.1. As L_1 increases even further,

¹⁴Phase diagrams are usually studied in thermodynamics, and we require, strictly speaking, the number of particles to be infinite. However, previous experience of analyzing quantum Hall systems has shown that even systems of very few particles provide a fairly accurate picture of the system in the thermodynamic limit.

¹⁵Again we disregard half of the states and just remember that there is a trivial twofold translational degeneracy of every state—hence this example implies also $|0101010101010101\rangle$.

this evolves continuously to states with other quantum numbers but with the same physics [7]. We can read from the phase diagram that the ground states at $\nu = 1/2$ are quite stable against perturbations of the interaction, since they remain the ground states for a while when the potential is varied.

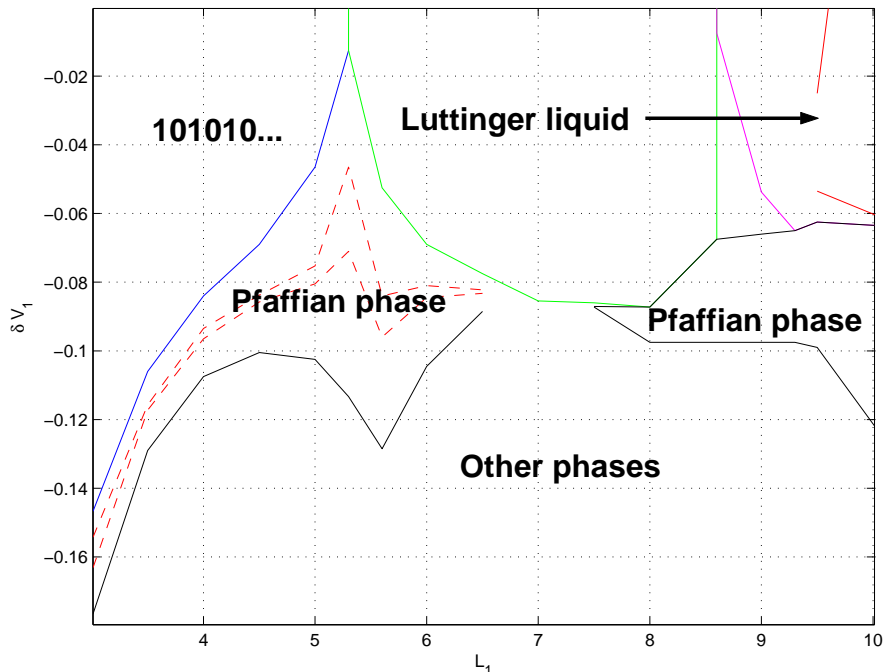


Figure 4.4: Phase diagram for half-filling on the torus as a function of L_1 and δV_1 , eight particles. Along the L_1 -axis we find the ground states of the ordinary Coulomb interaction in the lowest Landau level. The crystalline state $|1010\dots\rangle$ is separated from the Luttinger liquid by a phase transition. The Luttinger state evolves continuously to the bulk state as L_1 increases. For $\delta V_1 \neq 0$ other ground states appear. Within the solid lines in the center of the diagram, we find the pfaffian states. Within the dashed line these states are almost degenerate (their energy difference is less than 10% of the gap to the next state).

As we decrease the pseudopotential parameter from zero we eventually get to a regime where the pfaffian states are those with lowest energies—this area is labeled 'Pfaffian phase' in Fig. 4.4. Within the dashed lines the pfaffian states are even almost degenerate—their energies differ by less than 10% of the energy gap to the next state. One can note from the phase diagram that the pfaffian phase does not seem to be as stable as the $\nu = 1/2$ phase under changes in the interaction (at least not if one only considers the regime where the six ground states are close to degenerate).

Note also that we reach the pfaffian phase much earlier around the $\nu = 1/2$ phase transition than on the very thin torus in the leftmost part of the diagram. This is explained by the fact that, at the phase transition, both the TT state $|1010\dots\rangle$ and the XY-phase with states with the same quantum numbers as the pfaffian states $|1100\dots\rangle$ have low energy. Hence, we do not have to change the potential very much to reach a regime where these states are degenerate. On the very thin torus on the other hand, we know that the TT description also in the second Landau level only allows the states $|1010\dots\rangle$, and not $|1100\dots\rangle$. Thus, as the torus becomes thinner, we have to change the interaction more to find the pfaffian phase.

As L_1 increases, one can follow the pfaffian phase as it evolves to the larger system. Between approximately $L_1 = 7$ and $L_1 = 7.5$ we have not been able to find values of δV_1 where all the pfaffian states are the lowest energy states. In this regime other states compete for these positions. However, at even larger circumferences the pfaffian states take over again. By adding other pseudopotential parameters than δV_1 one should be able to find the pfaffian phase for all values of L_1 and hence see that it evolves continuously to the bulk state¹⁶. However, this remains to be investigated. From now on, we will only discuss what happens in the pfaffian phase on the thin torus (specifically up to $L_1 \sim 7$).

The pfaffian phase

The first thing we need to clarify here is: How do we know that it is the pfaffian phase we find when we decrease δV_1 like in Fig. 4.4? In section 4.3.1 we said that the crystalline states that minimize a repulsive three-body interaction at half-filling are of the kind $|10101010\dots\rangle$ and $|11001100\dots\rangle$ when $L_1 \rightarrow 0$. For $N_e = 8$ they are

$$\begin{aligned} &|1010101010101010\rangle, \\ &|0110011001100110\rangle + |1001100110011001\rangle, \\ &|0110011001100110\rangle - |1001100110011001\rangle, \end{aligned}$$

and the states obtained by acting with the translation operator T_2 on these states. This is the manifestation of the sixfold degeneracy of the pfaffian ground states on the torus, and one can actually show that the quantum numbers above are those of the pfaffian wave function [13]. Taking the limit $L_1 \rightarrow 0$ of the pfaffian, one arrives at the states above.

¹⁶Preliminary computer simulations for $N_e = 6$ indicate that this is not needed for this smaller system.

For non-vanishing values of L_1 , the hopping terms are non-zero, hence the low energy states will be superpositions of many different lattice crystals. However, their symmetries and hence their quantum numbers remain unchanged. As argued earlier, this makes it profitable to first focus on the thin torus, where we can think of the crystalline states as 'parents' of the pfaffian states in the bulk. In the regime labeled pfaffian phase in the diagram, these are the ground states of the hamiltonian.

Let us now investigate the properties of the pfaffian states as expressed in the lattice language.

Fractional charges

In section 3.3.2 we discussed how fractional charges form in a crystalline state. We concluded that adding a hole (site) to the $\nu = 1/2$ ground state in the thin limit changes the charge density at that position by $+e/2$. The question is: If we add one hole to the pfaffian phase, will we be able to see how this extra charge density splits into two fractional charges $+e/4$? We have investigated this by looking at the ground states of $N_e = 8$, $N_s = 17$, i.e. half-filling plus an extra hole, in the pfaffian regime. Plotting the average particle density of the ground state gives a clear picture of the fractional charges especially in the thin limit (see Fig. 4.5). From the density profile, one can see that in this limit the state has the crystalline form

$$|0110011\underline{0010}101\underline{010}\rangle.$$

Clearly, the ground state at filling $8/17$ consists of alternating domains of the lattice configurations $|01010101\dots\rangle$ and $|01100110\dots\rangle$. This mixing is possible thanks to the very small difference in energy of these states in the pfaffian regime (recall that it is already stated that degeneracy is required for the appearance of non-abelian statistics).

At the interfaces, the so-called domain walls, between the two types of crystalline states, there are concentrations of positive charge (blue color and underlined in the sequence). The added hole with charge $e/2$ has split into two $e/4$ charges!¹⁷ In this way the fractional charges appear as domain walls between the states $|01010101\dots\rangle$ and $|01100110\dots\rangle$. The interesting thing to note from the density plot is that this picture of the origin of the fractional

¹⁷An alternative way to see this, which will be generalized in chapter 6, is to realize that every string of four consecutive sites in the background ground states contains exactly two particles, i.e. the charge density is $-2e/4$. At the domain walls however, one single string of four sites instead contains one particle (charge density $-e/4$). Hence, the change in charge concentration in this deviating string is $e/4$.

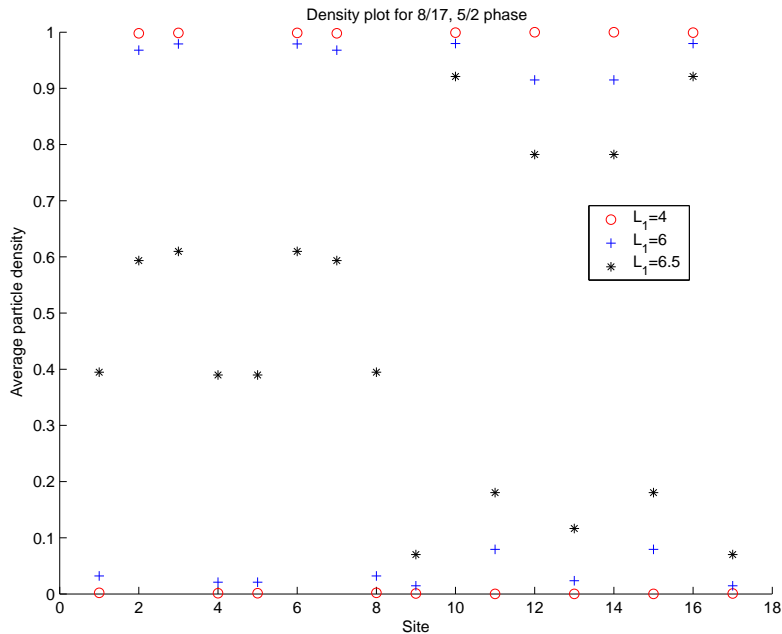


Figure 4.5: Plot of the average particle density at different sites. The filling fraction is $8/17$, i.e. we have added one hole to the half-filled system. The pseudopotential parameter is chosen to be in the pfaffian regime. In the plot one can see how two fractional charges form in the domain walls between the two types of crystalline states. The density configuration seemingly evolves continuously as L_1 increases.

charges seems to hold also for the thicker torus. Indeed, the change in the particle density of the ground state as L_1 increases indicates that it evolves continuously to the larger system (Fig. 4.5).

We have also searched for fractional charges in the low-lying spectrum at $N_e = 8$, $N_s = 16$ in the pfaffian regime. One expects, since the positively and negatively charged quasiparticles attract each-other, that the lowest states will keep these charges close together while they will become more separate in higher excitations. The computer simulations give that the first excited states are of the kind

$$|1010\underline{10110010}1010\rangle,$$

with a 32-fold degeneracy (16 T_2 translations times two because of a mirror symmetry). These states allow for two different interpretations. Either one may see it as the state $|101010\dots\rangle$ but with one electron moved one step (fractional charges $+e/2$ and $-e/2$ beside each-other). Or, one can see it

as a string of $|1010\dots\rangle$ connected to a short sequence of $|0011\dots\rangle$ and two quarter charges very close to each-other in the domain walls (red and blue underlined). A similar situation holds for the second excited states, which look like

$$|0110011\underline{0010}\underline{1011}0\rangle$$

and have a 32-fold degeneracy. The difference is that now the background is of the kind $|11001100\dots\rangle$. In the third excited states, however, the quarter charged quasiparticles are more evident. These states,

$$|\underline{1011}0011\underline{0010}1010\rangle$$

(32-fold degeneracy) clearly consist of alternating strings $|1010\dots\rangle$ and $|1100\dots\rangle$. As expected, $-e/4$ (red underlined) and $+e/4$ (blue underlined) charges appear as domain walls.

The domain wall picture of fractional charges is more general than this, as will be explained in chapter 6.

Chapter 5

Spin chain description of bosons at $\nu = 1$

The quantum Hall systems treated so far in this thesis have been fermionic. The wave functions have been antisymmetric, we have only allowed for one particle on each lattice site and the hamiltonian in equation (3.25) does not contain hopping of two particles to or from the same site. However, a somewhat unexpected mathematical connection will now take us from the two-dimensional electron gas to rotating Bose-Einstein condensates (BEC's), and we will investigate the latter in the same manner as earlier the electrons—on the thin torus. We will map the bosonic system at filling $\nu = 1$ onto a spin-1/2 chain, just as we did for fermions at half-filling, and analyze the spin hamiltonian to argue why this system realizes a pfaffian phase.

5.1 How bosons enter the quantum Hall effect

Some ten years ago it was realized that there is an intimate connection between fermions in the quantum Hall system on the one hand, and neutral bosons in rapidly rotating Bose-Einstein condensates on the other [10, 11]¹. It turns out that the hamiltonians of the two cases are mathematically equivalent, and so the analysis of the two seemingly very different systems can be unified. Strong magnetic field for fermions here corresponds to high rotational frequency of the BEC.

Experimentally, much progress has been made in this area during the last decade. Very fast rotation speeds have revealed fascinating properties of the rotating condensates—the most striking being regular vortex lattices piercing the samples. However, to get into the quantum Hall regime (lowest Landau

¹For a nice review of the subject, see [45].

level), even higher frequencies are required—so high that the condensate clouds easily escape the confining potential and fly apart. To this day this problem is not solved, although the experiments are very close. This however does not prevent further theoretical progress. Let us see how this system can be treated in the lattice model.

Since we are dealing with bosons, we must remember that interchanging two particles gives a plus sign, as opposed to the fermion case. Also, we have the possibility for two particles to hop to or from the same site. Equation (3.25) and (3.26) hence translate into

$$\begin{aligned}
H &= \sum_i \sum_{|m| \leq k \leq N_s/2} V_{km} b_{i-k}^\dagger b_{i+m}^\dagger b_{i-k+m} b_i = \\
&= \sum_i \sum_{0 \leq m \leq k \leq N_s/2} V_{km} b_{i-k}^\dagger b_{i+m}^\dagger b_{i-k+m} b_i + h.c. \equiv \sum_{0 \leq m \leq k \leq N_s/2} \hat{V}_{km} \quad (5.1)
\end{aligned}$$

and

$$\begin{aligned}
V_{km} &= \frac{1}{2^{\delta_{k,m}(1+\delta_{k,0})} 2^{\delta_{k,N_s/2}}} (V_{i+m,i+k,i+m+k,i} + V_{i+m,i+k,i,i+m+k} \\
&\quad + V_{i+k,i+m,i,i+m+k} + V_{i+k,i+m,i+m+k,i}). \quad (5.2)
\end{aligned}$$

Another important difference is that, for bosons, no Landau level is ever filled or inert because many bosons may occupy the same single-particle state. For the same reason, provided that the rotational frequency of the sample is high enough, only the LLL will be occupied even for $\nu > 1$. Considering these facts we may now seek a quantum Hall description of the rotating bosons.

5.1.1 Connection between bosons and fermions at different fillings

There is a connection between bosons and fermions at different filling fractions, which can be explained in terms of Laughlin functions and Jastrow factors. There is a bosonic counterpart of the Laughlin wave function [4], namely $\Psi_{\nu=\frac{1}{2m}} \sim J^{2m}$, where $J = \prod_{i < j} (z_i - z_j)$ is the Jastrow factor. Note that this state is symmetric in the particle coordinates. Now multiply the wave function by another Jastrow factor. What happens is that the filling changes; $\nu = \frac{1}{2m} \rightarrow \frac{1}{2m+1}$, and the wave function becomes fermionic since the Jastrow factor is antisymmetric. We have gone from bosons at filling $\nu = \frac{1}{2m}$ to fermions at filling $\nu = \frac{1}{2m+1}$. In analogy with this one would find it probable to find similarities between for example fermions at filling $\nu = 1/2$ and bosons at filling $\nu = 1$. However, whereas the fermionic system as we know

realizes a gapless metallic state, the bosonic counterpart rather seems to be described by a threefold degenerate pfaffian Moore-Read wave function [8] (more similar to fermions at $\nu = 5/2$). This has been indicated by numerical studies². Below, we will now make use of the thin torus geometry in an attempt to understand this discrepancy on an analytical, microscopical level.

5.2 Mapping of $\nu = 1$ onto 1D spin-1/2 chain

In the previous chapter we mapped a half-filled Landau level onto a spin-1/2 chain, leading to a simplified view of $\nu = 1/2$ and $\nu = 5/2$. Here we will apply the same mapping (although in a bit more complicated manner) to bosons at filling $\nu = 1$. Just as before this requires a specific choice of Hilbert subspace, which we will call \mathcal{H}'_b .

5.2.1 The subspace and mapping rules

Consider only states where every n consecutive sites contain from $n - 1$ to $n + 1$ particles. Hence, states where a single site hosts more than two particles are not allowed. Neither are states which contain strings of the kind 011...10 and 211...12, where the number of ones in the string can be 0, 1, Note that this restriction is favorable from an electrostatic point of view. Now let every site n_i in the original boson state split into two new sites n'_{2i-1}, n'_{2i} on which the number of particles divide;

$$\begin{cases} n_i = 2 & \rightarrow n'_{2i-1}, n'_{2i} = 11 \\ n_i = 0 & \rightarrow n'_{2i-1}, n'_{2i} = 00 \\ n_i = 1 & \rightarrow n'_{2i-1}, n'_{2i} = 10 \text{ or } 01. \end{cases}$$

The mapping of $n = 1$ is uniquely defined by the location of the zeros and twos in the lattice state. If a 1 is to the right of a 2 (0), it will be mapped like $n_i = 1 \rightarrow n_{2i-1}, n_{2i} = 01$ (10). Furthermore, all neighboring 1's will be mapped in the same way. Finally, let the state $|1111\dots\rangle \rightarrow |01010101\dots\rangle \equiv |10101010\dots\rangle$ for completeness. An example is (remember the periodic boundary conditions):

$$|112111011\rangle \rightarrow |101011010101001010\rangle. \quad (5.3)$$

²See [46, 47, 48]. Results from our computer analysis gives the overlap ≈ 0.99 between the exact diagonalization and the MR wave function, while ≈ 0.92 for the gapless Rezayi-Read function, $N_s = 6$, $L_1 = 4$, Coulomb interaction. Similar results are obtained for delta interaction.

First note that these "new" lattice states obviously have filling fraction one half. Then realize, that they fulfill the restriction that every pair of sites $2i, 2i + 1$ ($i = 1, 2, \dots$) contains exactly one particle. We are hence back at the fermionic subspace for half-filling except for one thing—the alternative choice of sites, $2i - 1, 2i$, does not work here because $n'_{2i-1}, n'_{2i}=11$ around a 2, and 00 around a 0. Now we will make the mapping complete by letting

$$\begin{cases} n'_{2i}, n'_{2i+1} = 10 & \rightarrow s_i^z = \uparrow \\ n'_{2i}, n'_{2i+1} = 01 & \rightarrow s_i^z = \downarrow \end{cases}$$

as before. In other words, $s_i^z = \frac{1}{2}(n'_{2i} - n'_{2i+1})$. One may quickly realize that domain walls between spin polarized sections arise where there were zeros and twos in the original boson states. The same example as in (5.3) becomes:

$$|112111011\rangle \rightarrow |\downarrow\downarrow\uparrow\uparrow\uparrow\uparrow\downarrow\downarrow\rangle. \quad (5.4)$$

Correspondingly, every given spin chain is uniquely mapped onto a boson state by reversing the argument;

$$\begin{cases} s_i^z = \uparrow & \rightarrow n'_{2i}, n'_{2i+1} = 10 \\ s_i^z = \downarrow & \rightarrow n'_{2i}, n'_{2i+1} = 01 \end{cases}$$

or equivalently $n'_{2i} = \frac{1}{2} + s_i^z$, $n'_{2i+1} = \frac{1}{2} - s_i^z$. And then

$$\begin{cases} n'_{2i-1}, n'_{2i} = 11 & \rightarrow n_i = 2 \\ n'_{2i-1}, n'_{2i} = 00 & \rightarrow n_i = 0 \\ n'_{2i-1}, n'_{2i} = 10 \text{ or } 01 & \rightarrow n_i = 1. \end{cases}$$

The three last equations may be summarized like

$$n_i = n'_{2i-1} + n'_{2i} = 1 + s_i^z - s_{i-1}^z. \quad (5.5)$$

So, now we have managed to transfer the supposedly low-energy sector of the full bosonic Hilbert space onto the same subspace that we had for fermions before³. But what about the hamiltonian? To make any progress we have to express at least the most important terms in (5.1) in terms of

³There is actually a way to achieve the spin space mapping directly, without passing the fermionic subspace. The trick is to define the spin of a site to be \downarrow (\uparrow) if the particle number increases (decreases) to the right. When there are several 1's in a row they all carry the same spin. And for the other way around, simply let $n_i = 1 + s_i^z - s_{i-1}^z$. One can easily check that this reproduces equation (5.4). This method is faster and simpler than the one described above, which on the other hand has a more obvious connection to $\nu = 1/2$ and also can be simpler to use when one translates the bosonic operators to spin language.

spin operators. But before we do that, let us first briefly comment on how relevant the (spin) subspace \mathcal{H}'_b turns out to be for the low-energy physics.

It is obvious that on the thick torus, hopping will make contributions from states outside of the subspace too large for it to be a good approximation. But on the thin torus on the other hand, there is a good chance of high agreement between the ground state of the full Hilbert space and the ground state of the hamiltonian restricted to \mathcal{H}'_b . When the torus circumference goes to zero, the overlap between the two tends to 1, because the TT state $|1111\dots\rangle$ belongs to \mathcal{H}'_b . It then remains very high at least up to $L_1 = 6$, where it is 0.962 for Coulomb and 0.968 for delta interaction and $N_s = 8$. This is past the point where the phase transition between the TT state and the pfaffian phase occurs, as will be described later. This is true also for the ground states at $L_1 \sim 4$, where the overlap between the full Hilbert space and the subspace reaches 0.999 for both Coulomb and delta interaction, $N_s = 8$.

5.2.2 Spin operator hamiltonian

To find the spin version of a truncated bosonic hamiltonian turns out to be a bit more complicated than for fermions at half-filling. Partly because it includes the terms \hat{V}_{km} that are absent for fermions, but especially since the mapping of the boson states is non-local in the sense that the spin corresponding to $n_i = 1$ can depend on the particle number many sites away. Hence, entire domains of spins may be flipped by shifting the particle number on one single site. Also, the fact that the particle number on a site can be 2 for bosons, and not only 0 or 1, complicates matters. However, after using the constraint that both the initial and the final states must lie within \mathcal{H}'_b , the key equation (5.5) and some thinking of course, one reaches the following results⁴:

$$\begin{aligned} \hat{V}_{km} &= 2^{-\delta_{km}(1-\delta_{m,N_s/2})/2} V_{km} \sum_i s_{i-k}^+ \dots s_{i-k+m-1}^+ s_i^- \dots s_{i+m-1}^- \\ &\times \sqrt{\frac{3}{2} - s_{i-k-1}^z} \sqrt{\frac{3}{2} + s_{i-k+m}^z} \sqrt{\frac{3}{2} - s_{i-1}^z} \sqrt{\frac{3}{2} + s_{i+m}^z} + h.c., \quad m > 0. \end{aligned} \quad (5.6)$$

$$\hat{V}_{k0} = V_{k0} \sum_i \left(2s_i^z s_{i+k}^z - s_i^z s_{i+k-1}^z - s_i^z s_{i+k+1}^z \right). \quad (5.7)$$

The operators \hat{V}_{km} , $m > 0$, describe all hopping processes that occur *between two states within* \mathcal{H}'_b . Note that just like for fermions, the shortest

⁴Details on this can be found in the Appendix.

hopping— \hat{V}_{11} for bosons—corresponds to a nearest-neighbor spin flip. Here though, it comes with additional factors of s^z ;

$$\begin{aligned}\hat{V}_{11} &= \sqrt{2}V_{11} \sum_i \sqrt{\frac{3}{2} - s_{i-2}^z} \sqrt{\frac{3}{2} + s_{i+1}^z} (s_i^+ s_{i+1}^- + h.c.) = \\ &= V_{11} \sum_i \left(\frac{4 + 3\sqrt{2}}{4} + \frac{1}{\sqrt{2}}(s_{i+1}^z - s_{i-2}^z) + (4 - 3\sqrt{2})s_{i-2}^z s_{i+1}^z \right) \\ &\quad \times (s_{i-1}^+ s_i^- + h.c.).\end{aligned}\quad (5.8)$$

Here we have used the fact that $s_{i-1}^z = -1/2$ and $s_i^z = 1/2$ for $k = m$, and $(s_i^z)^2 = 1/4$. In general, the factors and terms containing s^z have their origin in the factors that appear when one acts with the bosonic operators b^\dagger and b on the states in \mathcal{H}'_b , see equation (5.1).

Like in the fermionic case treated in section 4.1.1, there are many processes that do not preserve the subspace, but they cannot be expressed in spin language and have to be left out here. Furthermore, unlike for fermions, the shortest hopping does not in general preserve \mathcal{H}'_b . For example, acting with \hat{V}_{11} on any pair of particles in $|1111\dots\rangle$ creates a site containing three particles, which is not allowed (actually, the TT state is special in the sense that *any hopping at all* takes it out of \mathcal{H}'_b). This means that the spin space might not be a good restriction even on the thin torus. However, as already mentioned we find large overlaps between \mathcal{H}_b and \mathcal{H}'_b after the transition from the state $|1111\dots\rangle$.

At this point it does not seem that we have gained very much by expressing the operators in spin language. However, it turns out that many of the terms above may be neglected and it is possible to write the bosonic spin hamiltonian in a way very similar to the fermionic in equation (4.3). One finds

$$\hat{H}'_b = \sum_i \sum_{k=1}^{N_s/2} \left[\frac{\alpha_k}{2} (s_i^+ s_{i+k}^- + h.c.) + \beta_k s_i^z s_{i+k}^z \right] + \mathcal{O}(s^3), \quad (5.9)$$

where

$$\beta_k = 2V_{k0} - (1 - \delta_{k,N_s/2} + \delta_{k+1,N_s/2})V_{k+1,0} - (1 + \delta_{k,1})V_{k-1,0}, \quad (5.10)$$

$$\alpha_1 = \frac{1}{2}(4 + 3\sqrt{2})V_{11} \quad (5.11)$$

and

$$\alpha_k = \frac{1}{8}(17 + 12\sqrt{2})V_{k1}, \quad k = 2, 3, \dots \quad (5.12)$$

Details on the approximations we do are found in part C. in the Appendix.

Analysis of dominating terms

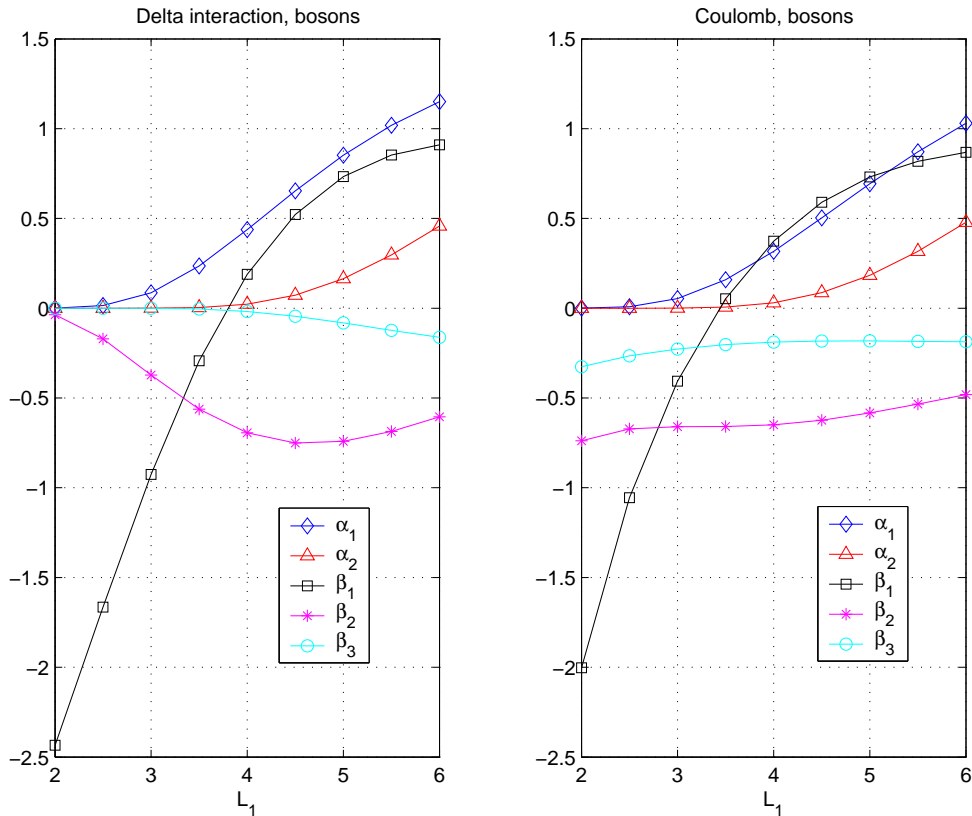


Figure 5.1: Here we show the values of the leading coefficients in the spin-chain hamiltonian for bosons with delta and Coulomb interaction respectively. The plot is constructed for $N_s = 10$, but changing the system size does not change the curves significantly.

In Figure 5.1 we have plotted the leading coefficients in equation (5.9), for delta and Coulomb interaction as a function of L_1 . We note that the hopping terms vanish as $L_1 \rightarrow 0$. Then when comparing these curves with Figure 4.1 and 4.3 we see the same tendency as for fermions in the second Landau level. When the circumference increases a bit from zero, the hopping coefficient α_1 is not obviously dominating⁵. Rather, the next nearest neighbor Ising term β_2 grows large.

⁵This is by the way a reason why the subspace is a good approximation on the thin torus.

How does this agree with what we already know about bosons at $\nu = 1$? Well, had $\beta_2 < 0$ been the only term in the hamiltonian,

$$\hat{H}'_b \sim \beta_2 \sum_i s_i^z s_{i+2}^z, \quad (5.13)$$

we would have had three exactly degenerate ground states

$$\begin{aligned} |1\rangle &= |\uparrow\uparrow\uparrow\uparrow \dots\rangle \equiv |\downarrow\downarrow\downarrow\downarrow \dots\rangle \\ |2\rangle &= |\downarrow\uparrow\downarrow\uparrow \dots\rangle \\ |\tilde{2}\rangle &= |\uparrow\downarrow\uparrow\downarrow \dots\rangle. \end{aligned}$$

Note especially that there are only three inequivalent states since the two spin-polarized states are mapped onto the same bosonic state and are thus equivalent by definition. Also, as opposed to $\nu = 5/2$, there is no second copy of the Hilbert space so there is only one version each of $|\downarrow\uparrow\downarrow\uparrow \dots\rangle$ and $|\uparrow\downarrow\uparrow\downarrow \dots\rangle$. Translating these states to boson number representation, we find

$$\begin{aligned} |1\rangle &= |1111\dots\rangle \\ |2\rangle &= |0202\dots\rangle \\ |\tilde{2}\rangle &= |2020\dots\rangle. \end{aligned}$$

These are the thin torus limits of the pfaffian Moore-Read wave function that is believed to describe $\nu = 1$ in the bulk. Furthermore, they are the three states with lowest energy within a range on the thin torus as is pictured in the phase diagram from exact diagonalization in \mathcal{H}_b in Figure 5.2. As the torus thickness increases from zero, the states $|2\rangle$ and $|\tilde{2}\rangle$ come closer in energy to the TT state $|1\rangle$, and these three are the lowest energy states from around $L_1 \sim 3.5$. At $L_1 \sim 3.8$, $|2\rangle$ and $|\tilde{2}\rangle$ pass the state $|1\rangle$ so that they are approximately degenerate. They seemingly then evolve continuously towards the thick torus as hopping terms take over.⁶

Like already stated at the end of section 5.2.1, the overlap between the full hamiltonian (with phase diagram like in the figure) and the subspace hamiltonian is high at least up to $L_1 = 6$. For larger circumferences the hopping terms start to take over so that the subspace no longer is a valid description of the low-energy states. Note that *any* hopping takes the state $|1\rangle = |1111\dots\rangle$ outside the subspace. Consequently, the overlap with this ground state becomes small earlier than the overlap with the hoppable states

⁶One should mention that the transition to the pfaffian phase is very unsharp compared to the (first-order) phase transition between the TT state and the XY-phase for fermions at $\nu = 1/2$. In the latter case, the TT state has quite high energy right after the transition, while it for $\nu = 1$ is one of the ground states even after the transition, and evolves together with the other pfaffian states as $L_1 \rightarrow \infty$.

$|2\rangle = |0202\dots\rangle$ and $|\tilde{2}\rangle = |2020\dots\rangle$. At around $L_1 \sim 6.5$, state $|1\rangle$ has evolved so that its largest contribution comes from $|10301030\rangle$ ($N_s = 8$), i.e. a state outside \mathcal{H}'_b which one gets by applying \hat{V}_{11} on $|11111111\rangle$.

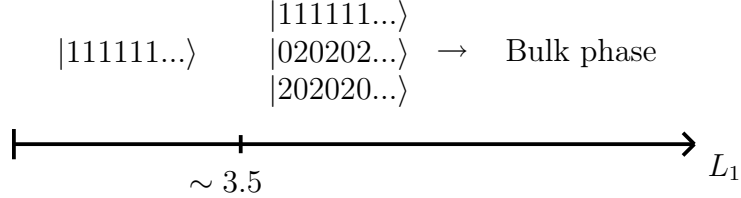


Figure 5.2: The phase diagram of bosons at $\nu = 1$ and Coulomb interaction as a function of L_1 .

To conclude, the very bold truncation in equation (5.13) is in good agreement with both the exact diagonalization and the expected Moore-Read ground states within a range of L_1 on the thin torus.

Fractional charges

The excitations at $\nu = 1$ are similar to the ones of $\nu = 5/2$, with the difference that the size of the fractional charges⁷ differs, which is evident from the mapping of the bosonic states.

As we know, the hamiltonian in (5.13) is minimized by states where all pairs of next nearest neighbors have the same spin. A minimal excitation is created by letting two pairs have opposite spins, which in turn is accomplished by constructing domain walls between the various ground states. For example, all states below have the same excitation energy $-\beta_2$ ⁸:

$$\begin{aligned} &| \uparrow \uparrow \uparrow \uparrow \uparrow \uparrow \uparrow \uparrow \uparrow \uparrow \downarrow \uparrow \uparrow \uparrow \uparrow \uparrow \uparrow \uparrow \uparrow \uparrow \uparrow \uparrow \rangle, \\ &| \uparrow \uparrow \uparrow \uparrow \uparrow \uparrow \uparrow \uparrow \downarrow \downarrow \downarrow \downarrow \uparrow \uparrow \uparrow \uparrow \uparrow \uparrow \uparrow \uparrow \uparrow \uparrow \rangle, \\ &| \uparrow \uparrow \uparrow \uparrow \uparrow \uparrow \uparrow \downarrow \downarrow \downarrow \downarrow \downarrow \downarrow \uparrow \uparrow \uparrow \uparrow \uparrow \uparrow \uparrow \uparrow \rangle. \end{aligned}$$

We of course get the same description of excitations as domain walls when we translate the above into number representation. Then it also becomes obvious that the excitations carry fractional charge $\pm \frac{e}{2}$, for example:

$$|11111111\underline{1}02020202\underline{1}11111111\rangle,$$

⁷Since the bosons in reality are neutral, this corresponds to fractional particle number in the experimental system.

⁸In the ground state, all pairs have energy $\beta_2/4$. Here, we have two pairs with opposite spin, each with energy $-\beta_2/4$. Hence the difference in energy compared to the ground state is $-\beta_2$.

where the blue (red) and underlined is a quasihole (quasiparticle).

These fractional charges are in agreement with what one gets from the bosonic pfaffian wave function [8]. We also find them in excited states, above the three (almost) degenerate ground states. As an example, let us present the result of the exact diagonalization studies at $L_1 = 3.8$, $N_s = 8$.

For delta interaction, the ground state ($E_0 = 0$) is the state $|11111111\rangle$. It is closely followed by $|20202020\rangle$ and $|02020202\rangle$ ⁹ ($E_1 \approx 0.01$ and $E_2 \approx 0.04$). After that there is a clear gap to the next excited states, consisting of mixtures of the three ground states. For example, states of the type $|11111120\rangle$ first appear at $E_3 \approx 0.40$, $|11202020\rangle$ at $E_9 \approx 0.49$ and $|1111020202\rangle$ at $E_{11} \approx 0.50$.

For Coulomb at this thickness, the ground state ($E_0 = 0$) is $|20202020\rangle$. Close to this state we find its translated version $|02020202\rangle$ and also $|11111111\rangle$ ($E_1 \approx 0.01$, $E_2 \approx 0.02$). Furthermore, $|11111120\rangle$ first appears at $E_3 \approx 0.60$, $|11202020\rangle$ at $E_5 \approx 0.65$ and $|1111020202\rangle$ at $E_{21} \approx 0.77$.

Note that the excitation energies approximately are of the order of $-\beta_2$ in this regime of L_1 , see Figure 5.1. One should also mention that the states given here are not completely crystalline since $L_1 \neq 0$. However, hopping contributions from other states are still small. For example, the ground state for delta interaction at $L_1 = 3.8$ above is $0.91|11111111\rangle + \dots$

⁹To be precise, expressed as eigenstates to the T_2 operator the states are $|20202020\rangle \pm |02020202\rangle$, and they are not exactly degenerate because hopping interaction is not completely vanishing.

Chapter 6

More on non-abelian quantum Hall states

6.1 Ground states and elementary excitations on the thin torus

We have seen examples on how elementary excitations are formed as domain walls between degenerate ground states on the thin torus. In this chapter we will generalize this to a large class of filling fractions and then just briefly state a strong connection with conformal field theory when counting the degeneracies of quasiparticles and -holes in non-abelian quantum Hall states¹. We will analyze the so-called Read-Rezayi (RR) states [49], which are candidates for describing the FQHE at filling $\nu = \frac{k}{kM+2}$, with M even describing bosons and M odd fermions. The RR wave functions are all ground states of a certain local $k + 1$ -body interaction, and on the thin torus, because of the suppressed hopping, this boils down to all clusters of $k + 1$ particles wanting to be as far apart as possible. For $M \neq 0$ it is true that one may not have more than one particle on M consecutive sites. However, we will focus on the $M = 0$ case (bosons) and later only state the generalization to other values of M .

6.1.1 Ground states

Consider a hamiltonian consisting of a repulsive $k + 1$ -body interaction, with no hopping as is the case on the thin torus. The interaction poses no restriction on how close any k particles may be, but having $k + 1$ closely lying

¹This chapter follows parts of the appended paper II, [15].

particles costs a lot of energy. On top of this we have a filling fraction $\nu = \frac{k}{2}$ ($M = 0$), i.e. on average we will have k particles per 2 sites. It is clear that a completely even spread in particle number is a good ground state candidate because it keeps any clusters of particles, and in particular any clusters of size $k + 1$, as separate as possible. For $k = 3$ for example, this would be the state $|121212\dots\rangle$. This state keeps any pair of particles away from each-other. But we have more freedom than that! The only thing we have to bother about is clusters of $k + 1$ particles, which is four in this case. The state $|303030\dots\rangle$ also keeps any four particles as separate as possible, and has thus the same low energy! One quickly realizes that in order to minimize the energy for a state of filling fraction $\nu = \frac{k}{2}$, we need only to have exactly k particles on any string of two consecutive sites (for $M \neq 0$ this generalizes to having k particles on $kM + 2$ consecutive sites). For general values of k this yields degenerate ground states of the kind

$$|k - l, l, k - l, l, \dots\rangle, \quad (6.1)$$

with $l = 0, 1, \dots, k$. Or, in other words, the states with unit cell $[k - l, l]$.²

What is the degeneracy of these states? Well, as long as N_s is even, all these states fulfill the periodic boundary conditions of the torus. And since there are $k + 1$ different values of l the degeneracy is $k + 1$ in this case. However, for N_s odd there is only one possibility, namely the state $[k/2, k/2]$, which only appears when k is even. To summarize: N_s even implies a degeneracy of $k + 1$. N_s odd, k even yields a degeneracy of one. N_s odd, k odd implies zero degeneracy.

We also state that for $M \neq 0$, this generalizes to $(k + 1)(kM + 2)/2$ when $2N_e/k = 0 \pmod{2}$, and $(kM + 2)/2$ when $2N_e/k = 1 \pmod{2}$.

6.1.2 Excitations

Now, let's try to find the smallest possible charge excitations for these states (the excitations will appear both in the first excited states at exact filling $\nu = \frac{k}{kM+2}$, and in the ground state configurations when the filling deviates slightly from those fractions). Recall that the ground states, minimizing the $k + 1$ -body interaction, were such that any string of two consecutive sites host exactly k particles. There are N_s such strings, one starting at each

²Remember that the $k + 1$ -body interaction is no more and no less than a good effective description of the two-body interaction between the particles of the real system. In the limit $L_1 \rightarrow 0$ we thus have the ordinary TT ground states. Hence, (6.1) is really not a true description of the torus ground states until after the phase transition to the non-abelian phase. However, the transition occurs on very thin tori, and we may still consider them as being parents of the bulk ground states.

site. One may realize, that the least change away from this pattern that one can achieve, is to let one single string carry $k \pm 1$ particles, while all other strings still host k particles. An example ($k = 3$) of this would be the state $|1212\underline{11}212\rangle$, where the underlined string has less charge than all other strings. In general, we can create these excitations by connecting different ground states. To make the following analysis more compact and clear, we will use the short-hand notation for each ground state. $k = 3$ will again serve as an example. Let each ground state be represented by its unit cell;

$$|030303\dots\rangle \rightarrow [03] \tag{6.2}$$

$$|121212\dots\rangle \rightarrow [12] \tag{6.3}$$

$$|212121\dots\rangle \rightarrow [21] \tag{6.4}$$

$$|303030\dots\rangle \rightarrow [30]. \tag{6.5}$$

The excitation in the example above may now be written $[12][21]$. Note that this notation does not contain any information on the length of the states, nor if the domain wall is of the type $|1212\underline{11}212\rangle$ (quasihole) or $|1212\underline{22}1212\rangle$ (quasiparticle). In general, constructing an elementary excitation is done by forming a domain wall between states with l differing by one. For quasiholes:

$$[k - l, l][k - l - 1, l + 1], \quad 0 \leq l < k, \tag{6.6}$$

and for quasiparticles:

$$[k - l, l][k - l + 1, l - 1], \quad 0 < l \leq k. \tag{6.7}$$

An obvious question to ask is: What is the fractional charge of the quasiholes and -particles? The answer is (for general M)

$$e^* = \pm \frac{e}{kM + 2}, \tag{6.8}$$

and there are several ways to arrive at this result. One is simply to compare the excitation charge with the background; in the ground state, the charge is ek per every $kM + 2$ sites. At the domain wall, however, the charge is $e(k \pm 1)$ per $kM + 2$ sites. The difference, $\pm \frac{e}{kM + 2}$ is the charge of the excitation. One may also use the Su-Schrieffer counting argument [33]. However, that method

requires introduction of a specific number of quasiholes/-particles. An easier procedure, that may be applied to generic filling fractions $\nu = \frac{p}{q}$ is presented here. In the ground state, the particle density is the same in all N_s strings. Hence, the total charge is

$$eN_e = N_s \frac{ek}{kM + 2}. \quad (6.9)$$

When excitations are added, the total charge changes to

$$eN_e = (N_s - n_{qp} - n_{qh}) \frac{ek}{kM + 2} + n_{qp} \frac{e(k+1)}{kM + 2} + n_{qh} \frac{e(k-1)}{kM + 2}, \quad (6.10)$$

where n_{qp} , n_{qh} are the number of quasiparticles and quasiholes respectively. We rewrite this equation to

$$eN_e = N_s \frac{ek}{kM + 2} + (n_{qp} - n_{qh}) \frac{e}{kM + 2}, \quad (6.11)$$

by which we readily confirm equation (6.8).

Another important issue is the degeneracy of the excited states, since it is crucial for the non-abelian statistics. The precise question we like to address is: What is the total torus degeneracy for a state with $n = n_{qh} + n_{qp}$ excitations, as a function of k , M and n ? The analysis is simplified by picturing the problem in a so-called Bratteli diagram as in Figure 6.1, here with $M = 0$. Each state, labeled by the *level* l may only be connected to states in the adjacent levels as explained above. Each transition between levels creates a quasihole or a quasiparticle. The degeneracy is the number of possible paths that yield the right number of excitations in question. Note that the degeneracy is dependent on whether N_s is even or odd, because of the periodic boundary conditions. If we for example start in state [12], we need to end with [12] ([21]) if N_s is even (odd).

Bratteli diagrams are well known in combinatorics, and we can thus steal some useful results from this area of mathematics, here presented without proofs. We introduce the off-diagonal adjacency matrix \mathbf{N}_1 ;

$$(N_1)_{ij} = \delta_{i,j+1} + \delta_{i,j-1}; \quad i, j = 0, \dots, k. \quad (6.12)$$

It follows that the number of ways to go from level l_1 to level l_2 via n excitations (i.e. domain walls) is given by

$$d(k, n, l_1, l_2) = (N_1^n)_{l_1 l_2}, \quad (6.13)$$

and the total degeneracy for n domain walls is

$$td(k, M = 0, n, \delta) = \sum_{paths} d(k, n, l_1, l_2) = Tr(\mathbf{N}_1^n \mathbf{B}^\delta), \quad (6.14)$$

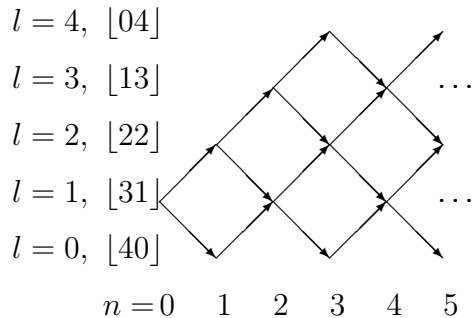


Figure 6.1: An example of a Bratelli diagram, here for $k = 4$. The arrows indicate how we can join different ground states to create the minimally charged excitations discussed in the text.

where \mathbf{B}^δ takes care of the periodic boundary conditions and whether N_s is even or odd; $\delta = 0$ or 1 when N_s is even or odd respectively. The off-diagonal permutation matrix \mathbf{B} is defined as $(B)_{ij} = \delta_{i,k-j}$; $i, j = 0, \dots, k$.

For $M \neq 0$ it turns out that only a minor modification is necessary. The degeneracy becomes

$$td(k, M, n, \delta) = \frac{kM + 2}{2} Tr(\mathbf{N}_1^n \mathbf{B}^\delta) \quad (6.15)$$

with $\delta = (2N_e + n_{qh} - n_{qp})/k \bmod 2$.

6.1.3 Connection to CFT

As mentioned earlier in this thesis, there is a strong mathematical connection between the fractional quantum Hall effect and certain classes of conformal field theories (CFT). For example, good trial wave functions for the FQHE have been constructed from CFT correlators, see e.g. [8]. It is a nice fact that the above degeneracies also can be derived using a CFT approach, in which they are calculated from the fusion rules. This interesting connection will however not be a subject of this thesis, and readers are referred to Paper II, [15], for details.

Chapter 7

Conclusions and outlook

We have investigated various quantum Hall systems on a thin torus. When the torus circumference L_1 is small, hopping is suppressed and the physics becomes more transparent. Within a certain regime on the thin torus, the low-energy sectors of three very different systems— $\nu = 1/2$ (fermions), $\nu = 5/2$ (fermions) and $\nu = 1$ (bosons)—may all be mapped onto 1D spin-1/2 chains. Expressed in spin language, truncated hamiltonians allow for simple analysis of the nature of these systems.

For fermions at filling $\nu = 1/2$, the truncated hamiltonian is dominated by the nearest-neighbor spin flip, as earlier found in [6]. Keeping only this term yields a solution in terms of neutral dipoles, giving a microscopic understanding of why this state is gapless.

At filling $\nu = 5/2$ the shortest spin flip no longer dominates the hamiltonian. Instead a negative next-nearest neighbor Ising term is found to be large. We note that diagonalizing the hamiltonian keeping only this interaction term produces sixfold degenerate ground states of type $|1100\dots\rangle$ and $|1010\dots\rangle$. Furthermore, it gives gapped fractionally charged excitations of size $\pm e/4$ emerging as domain walls between different ground states. All this is in agreement with what is expected from the pfaffian Moore-Read wave function describing $\nu = 5/2$.

The same Ising term seemingly dominates the hamiltonian for bosons at filling $\nu = 1$. In this case this translates into threefold degenerate ground states of type $|1111\dots\rangle$ and $|2020\dots\rangle$, as well as fractional charges of size $\pm e/2$. Again, this is in agreement with the properties of the bosonic Moore-Read wave function that is believed to describe this system.

In addition to the above we have used a pseudopotential expansion of the interaction potential at half filling to investigate the connection between $\nu = 1/2$ and $\nu = 5/2$. We find that the sixfold degenerate pfaffian ground states of the latter is present on the thin torus as expected. Numerics also

confirm the domain wall picture of the elementary excitations.

The domain wall excitations may be generalized to a large class of (bosonic and fermionic) filling fractions $\nu = \frac{k}{kM+2}$. Here the ground states are known to be eigenstates of repulsive $k+1$ -body interactions. On the thin torus this is manifested in crystalline states where any string of $kM+2$ sites are occupied by exactly k particles. A simple counting procedure shows that the size of the fractional charges is $\pm \frac{e}{kM+2}$. Furthermore, the degeneracy of states with a specific number of quasiparticles and -holes may be illustrated by so-called Bratteli diagrams and calculated using known combinatorics. The results agree with what is previously known from conformal field theory.

After our first paper on non-abelian quantum Hall states on the thin torus [13], there has been a number of extensions and reformulations of this work. Work with explicit references to the thin torus includes [50, 51, 34, 35, 52, 53, 54]. The same domain wall descriptions has also been obtained by other approaches [55, 56] and corroborates the picture that this lies at the heart of the structure of all known quantum Hall states. Moreover, more mathematically inclined people have confirmed that this picture also holds in the thermodynamic limit (for the Laughlin state) [57].

Summarizing, the results reported in this thesis, together with previous work by our group as well as the related work mentioned above has shown the profits of studying the quantum Hall system on the thin torus, and there are presumably more things to explore along this line. For example it would be interesting to see if other filling fractions (bosonic and fermionic) than the ones treated here may be mapped onto spin chains and analyzed in this geometry.

Appendix

A. Details on \hat{V}_{k0} in spin language

Here we fill in the details on how to derive the expressions for the electrostatic operators in equation (5.7). This is actually quite easy—just make use of the relation $n_i = 1 + s_i^z - s_{i-1}^z$ and $(s_i^z)^2 = 1/4$. For $k \neq 0$ we have

$$\begin{aligned}
 \hat{V}_{k0} &= V_{k0} \sum_i b_i^\dagger b_{i-k}^\dagger b_{i-k} b_i = V_{k0} n_i n_{i-k} \\
 &= V_{k0} \sum_i (1 + s_i^z - s_{i-1}^z)(1 + s_{i-k}^z - s_{i-k-1}^z) \\
 &= V_{k0} \sum_i (2s_i^z s_{i+k}^z - s_i^z s_{i+k-1}^z - s_i^z s_{i+k+1}^z) + \text{const.}
 \end{aligned} \tag{1}$$

Furthermore, for $k = 0$:

$$\begin{aligned}
 \hat{V}_{00} &= V_{00} \sum_i b_i^\dagger b_i^\dagger b_i b_i = V_{00} \sum_i n_i (n_i - 1) \\
 &= V_{00} \sum_i (1 + s_i^z - s_{i-1}^z)(s_i^z - s_{i-1}^z) = -2V_{00} \sum_i s_i^z s_{i+1}^z + \text{const.},
 \end{aligned} \tag{2}$$

which may be included in the expression for $k \neq 0$ above.

Dropping the unimportant constants one readily finds equation (5.7).

B. Details on \hat{V}_{km} in spin language

Here are some details on how to arrive at the expression for the hopping operators in equation (5.6). This is a bit tricky.

We want to find the spin operators that act in the same way as $\hat{V}_{km} = V_{km} \sum_i b_{i-k}^\dagger b_{i+m}^\dagger b_{i-k+m} b_i + h.c.$, $m \neq 0$, does on states within the subspace. Let us first consider the case $k \neq m$, i.e. when hopping involves four different

sites. We have:

$$\begin{aligned}
& \dots n_{i-k} \dots n_{i-k+m} \dots n_i \dots n_{i+m} \dots \\
& \quad \updownarrow \hat{V}_{km} \\
& \dots n_{i-k} + 1 \dots n_{i-k+m} - 1 \dots n_i - 1 \dots n_{i+m} + 1 \dots
\end{aligned}$$

where n_{i-k+m} and n_i may be 1 or 2, and n_{i-k} and n_{i+m} may be 0 or 1.

Now use the fact that both the initial and the final state must lie within \mathcal{H}'_b . The number of particles in the string including site $i - k + m$ and i changes by two in the hopping process. Hence we must have

$$\begin{aligned}
& \dots \underbrace{n_{i-k+m} \dots n_i}_{n+1 \text{ particles on } n \text{ sites}} \dots \longleftrightarrow \dots \underbrace{n_{i-k+m} - 1 \dots n_i - 1}_{n-1 \text{ particles on } n \text{ sites}} \dots
\end{aligned}$$

Now analyze the different cases. Consider the example $n_{i-k+m} = n_i = 2$. To fulfill the requirement of $n + 1$ particles on n sites in the leftmost state, we must have one extra 0 between site $i - k + m$ and i . Besides this 0 we may also have additional pairs of zeros and twos, but no 2 to the right (left) of n_{i-k+m} (n_i). Ones may be inserted anywhere without changing the spins of the important sites. We may now sketch the situation further:

$$\begin{aligned}
& \dots n_{i-k} \dots \underset{i-k+m}{2} \dots 0 \dots \underset{i}{2} \dots n_{i+m} \dots \\
& \quad \updownarrow \\
& \dots n_{i-k} + 1 \dots \underset{i-k+m}{1} \dots 0 \dots \underset{i}{1} \dots n_{i+m} + 1 \dots
\end{aligned}$$

Further, from the above and the subspace rules we find that there can only be 1's between n_{i-k} and n_{i-k+m} , and between n_i and n_{i+m} respectively. Finally, we will translate the hopping process in terms of spins via the fermionic subspace:

$$\left\{ \begin{array}{l}
\dots n_{i-k} \ 1 \dots \underset{i-k+m}{1} \ \underset{i-k+m}{2} \ 1 \dots 0 \dots 1 \ \underset{i}{2} \ 1 \dots 1 \ n_{i+m} \dots \\
\dots \underbrace{0/1 \ 0 \ 1 \ 0 \dots 1 \ 0 \ 1 \ 1 \ 0 \ 1 \dots 0 \ 0 \dots 1 \ 0 \ 1 \ 1 \ 0 \ 1 \dots 0 \ 1 \ 0 \ 0/1 \dots}_{n_{i-k}} \dots \underbrace{\dots}_{n_{i+m}} \dots \\
\dots (\uparrow / \downarrow) \underbrace{\downarrow \downarrow \dots \downarrow \downarrow}_{i-k+m} \uparrow \ \uparrow \dots \uparrow \downarrow \dots \downarrow \downarrow \underbrace{\uparrow \uparrow \dots \uparrow \uparrow}_i (\downarrow / \uparrow) \dots
\end{array} \right.$$

\updownarrow

$$\left\{ \begin{array}{l} \dots n_{i-k} + 1 \quad 1 \quad \dots \quad 1 \quad \underline{1} \quad 1 \quad \dots \quad 0 \quad \dots \quad 1 \quad \underline{1} \quad 1 \quad \dots \quad 1 \quad n_{i+m} + 1 \dots \\ \dots \underbrace{0/1 \quad 1 \quad 0 \quad 1 \dots 0 \quad 1 \quad 0 \quad 1 \quad 0 \quad 1 \dots 0 \quad 0 \dots 1 \quad 0 \quad 1 \quad 0 \quad 1 \quad 0 \dots 1 \quad 0 \quad 1 \quad 0/1 \dots}_{n_{i-k}+1} \underbrace{\dots}_{n_{i+m}+1} \dots \\ \dots (\uparrow / \downarrow) \underbrace{\uparrow \uparrow \dots \uparrow \uparrow}_{i-k+m} \uparrow \quad \uparrow \dots \uparrow \downarrow \dots \downarrow \downarrow \underbrace{\downarrow \downarrow \dots \downarrow \downarrow}_i (\downarrow / \uparrow) \dots \end{array} \right.$$

The spins at site $i - k - 1$ and $i + m$ is decided by whether n_{i-k-1} , n_{i+m} are one or zero. However, the underlined colored spins are the only spins changing in the process, and we find that

$$b_{i-k}^\dagger b_{i+m}^\dagger b_{i-k+m} b_i \propto s_{i-k}^+ \dots s_{i-k+m-1}^+ s_i^- \dots s_{i+m-1}^- \quad (3)$$

This is true also for the other choices of n_{i-k+m} , n_i , and also for $k = m$.

It remains to calculate the correct proportionality factor in (3)... For $k \neq m$ and hopping "outwards" we have:

$$\begin{aligned} V_{km} b_{i-k}^\dagger b_{i+m}^\dagger b_{i-k+m} b_i | \dots n_{i-k} \dots n_{i-k+m} \dots n_i \dots n_{i+m} \dots \rangle = \\ = V_{km} \sqrt{n_{i-k} + 1} \sqrt{n_{i-k+m}} \sqrt{n_i} \sqrt{n_{i+m} + 1} \\ \times | \dots n_{i-k} + 1 \dots n_{i-k+m} - 1 \dots n_i - 1 \dots n_{i+m} + 1 \dots \rangle. \end{aligned} \quad (4)$$

Using $n_i = 1 + s_i^z - s_{i-1}^z$ we realize that we get the correct factors from¹

$$\begin{aligned}
& V_{km} s_{i-k}^+ \dots s_{i-k+m-1}^+ s_i^- \dots s_{i+m-1}^- \sqrt{2 + s_{i-k}^z - s_{i-k-1}^z} \\
& \times \sqrt{1 + s_{i-k+m}^z - s_{i-k+m-1}^z} \sqrt{1 + s_i^z - s_{i-1}^z} \sqrt{2 + s_{i+m}^z - s_{i+m-1}^z} \\
& \times |\dots \downarrow_{i-k} \dots \downarrow_{i-k+m-1} \dots \uparrow_i \dots \uparrow_{i+m-1} \dots\rangle = \\
& = V_{km} s_{i-k}^+ \dots s_{i-k+m-1}^+ s_i^- \dots s_{i+m-1}^- \\
& \times \sqrt{\frac{3}{2} - s_{i-k-1}^z} \sqrt{\frac{3}{2} + s_{i-k+m}^z} \sqrt{\frac{3}{2} - s_{i-1}^z} \sqrt{\frac{3}{2} + s_{i+m}^z} \\
& \times |\dots \downarrow_{i-k} \dots \downarrow_{i-k+m-1} \dots \uparrow_i \dots \uparrow_{i+m-1} \dots\rangle. \quad (5)
\end{aligned}$$

One may convince oneself that the hermitian conjugate produces the same factors, so that for $k \neq m > 0$

$$\begin{aligned}
\hat{V}_{km} &= V_{km} \sum_i s_{i-k}^+ \dots s_{i-k+m-1}^+ s_i^- \dots s_{i+m-1}^- \\
& \times \sqrt{\frac{3}{2} - s_{i-k-1}^z} \sqrt{\frac{3}{2} + s_{i-k+m}^z} \sqrt{\frac{3}{2} - s_{i-1}^z} \sqrt{\frac{3}{2} + s_{i+m}^z} + h.c.. \quad (6)
\end{aligned}$$

The proportionality factors need to be corrected a little when $k = m$ (i.e. $i - k + m = i$), because of the bosonic factors. Also, $k = m = N_s/2$ yields further corrections to the above since $i - k = i + m$ in that case. In the end, we may write

$$\begin{aligned}
\hat{V}_{km} &= 2^{-\delta_{km}(1-\delta_{m,N_s/2})/2} V_{km} \sum_i s_{i-k}^+ \dots s_{i-k+m-1}^+ s_i^- \dots s_{i+m-1}^- \\
& \times \sqrt{\frac{3}{2} - s_{i-k-1}^z} \sqrt{\frac{3}{2} + s_{i-k+m}^z} \sqrt{\frac{3}{2} - s_{i-1}^z} \sqrt{\frac{3}{2} + s_{i+m}^z} + h.c., \quad m > 0. \quad (7)
\end{aligned}$$

This is equation (5.6).

C. Spin hamiltonian \hat{H}'_b

Here we explain how we motivate the truncated spin hamiltonian for bosons in equation (5.9).

¹Remember that n_{i-k} , n_{i-k+m} , n_i and n_{i+m} refer to the initial state, hence s_{i-k}^z , $s_{i-k+m-1}^z$, s_i^z and s_{i+m-1}^z , which do not commute with the spin-flip operators, must stand to the right of these.

First, on the thin torus, V_{km} for large m are very small—one can show that as $L_1 \rightarrow 0$, $V_{km} \sim e^{-2\pi^2 m^2/L_1^2} V_{k0}$. Hence, as a first approximation we discard all terms but \hat{V}_{k0} and \hat{V}_{k1} in the hamiltonian;

$$\hat{H}'_b = \sum_{k=0}^{N_s/2} \hat{V}_{k0} + \sum_{k=1}^{N_s/2} \hat{V}_{k1}. \quad (8)$$

The sum over \hat{V}_{k0} may be evaluated directly from equation (5.7);

$$\begin{aligned} \sum_{k=0}^{N_s/2} \hat{V}_{k0} &= \sum_i \sum_{k=0}^{N_s/2} V_{k0} (2s_i^z s_{i+k}^z - s_i^z s_{i+k-1}^z - s_i^z s_{i+k+1}^z) = \\ &= \sum_i \left\{ 2 \sum_{k=1}^{N_s/2} V_{k0} - \sum_{k=-1}^{N_s/2-1} V_{k+1,0} - \sum_{k=1}^{N_s/2+1} V_{k-1,0} \right\} s_i^z s_{i+k}^z + \text{const.} = \\ &= \sum_i \left\{ \sum_{k=1}^{N_s/2} (2V_{k0} - V_{k+1,0} - V_{k-1,0}) s_i^z s_{i+k}^z + \right. \\ &\quad \left. -V_{00} s_i^z s_{i+1}^z + V_{N_s/2+1,0} s_i^z s_{i+N_s/2}^z - V_{N_s/2,0} s_i^z s_{i+N_s/2-1}^z \right\} + \text{const.} = \\ &= \sum_i \sum_{k=1}^{N_s/2} \underbrace{\left[2V_{k0} - (1 - \delta_{k,N_s/2} + \delta_{k,N_s/2-1}) V_{k+1,0} - (1 + \delta_{k,1}) V_{k-1,0} \right]}_{\beta_k} s_i^z s_{i+k}^z, \end{aligned}$$

where we dropped the unimportant constant in the last step, and we have found the electrostatic β_k terms in (5.9).

The hopping part of the truncated spin hamiltonian is a bit trickier to calculate... From (5.6) we see that

$$\hat{V}_{11} = \sqrt{2} V_{11} \sum_i s_{i-1}^+ s_i^- \sqrt{\frac{3}{2} - s_{i-2}^z} \sqrt{\frac{3}{2} + s_{i+1}^z} + h.c. \quad (9)$$

and

$$\hat{V}_{k \neq 1,1} = V_{k1} \sum_i s_{i-k}^+ s_i^- \sqrt{\frac{3}{2} - s_{i-k-1}^z} \sqrt{\frac{3}{2} + s_{i-k+1}^z} \sqrt{\frac{3}{2} - s_{i-1}^z} \sqrt{\frac{3}{2} + s_{i+1}^z} + h.c..$$

It is possible to simplify these expressions by first Taylor expanding the roots, using $(s_i^z)^2 = \frac{1}{4}$. One finds that

$$\sqrt{\frac{3}{2} \pm s_i^z} = a \pm b s_i^z, \quad (10)$$

where $a = \frac{1+\sqrt{2}}{2} \approx 1.2$ and $b = 1 - \sqrt{2} \approx -0.4$. In other words,

$$\hat{V}_{11} = \sqrt{2}V_{11} \sum_i s_{i-1}^+ s_i^- (a^2 + ab(s_{i+1}^z - s_{i-2}^z)) + \mathcal{O}(s^4) + h.c. \quad (11)$$

and

$$\hat{V}_{k \neq 1, 1} = V_{k1} \sum_i s_{i-k}^+ s_i^- (a^4 + a^3 b (s_{i-k+1}^z - s_{i-k-1}^z - s_{i-1}^z + s_{i+1}^z)) + \mathcal{O}(s^4) + h.c..$$

The contributions from $\mathcal{O}(s^4)$ are in both cases negligible because b is small compared to a . We also note that the coefficients in front of the terms of order s^3 are about a third of the α_k coefficients multiplying $s_{i-k}^+ s_i^-$. Had α_k been large in comparison with β_k on the thin torus, we would have had to consider these cubic terms. However, this is not the case as can be seen in Figure 5.1. We conclude that

$$\begin{aligned} \hat{V}_{11} &= \sqrt{2}a^2 V_{11} \sum_i s_{i-1}^+ s_i^- + \mathcal{O}(s^3) + h.c. = \\ &= \frac{\alpha_1}{2} \sum_i s_{i-1}^+ s_i^- + \mathcal{O}(s^3) + h.c., \end{aligned} \quad (12)$$

where

$$\alpha_1 = 2\sqrt{2}a^2 V_{11} = \frac{1}{2}(4 + 3\sqrt{2})V_{11}. \quad (13)$$

We also have

$$\begin{aligned} \hat{V}_{k \neq 1, 1} &= a^4 V_{k1} \sum_i s_{i-k}^+ s_i^- + \mathcal{O}(s^3) + h.c. = \\ &= \frac{\alpha_k}{2} \sum_i s_{i-k}^+ s_i^- + \mathcal{O}(s^3) + h.c., \end{aligned} \quad (14)$$

with

$$\alpha_k = 2a^4 V_{k1} = \frac{1}{8}(17 + 12\sqrt{2}), \quad k > 1. \quad (15)$$

Summarizing, we have

$$\begin{aligned} \hat{H}'_b &= \sum_{k=0}^{N_s/2} \hat{V}_{k0} + \sum_{k=1}^{N_s/2} \hat{V}_{k1} = \\ &= \sum_i \sum_{k=1}^{N_s/2} \left[\frac{\alpha_k}{2} (s_i^+ s_{i+k}^- + h.c.) + \beta_k s_i^z s_{i+k}^z \right] + \mathcal{O}(s^3), \end{aligned} \quad (16)$$

where the coefficients α_k and β_k are given above. This is equation (5.9).

Bibliography

- [1] K.v. Klitzing, G. Dorda and M. Pepper, Phys. Rev. Lett. **45**, 494 (1980).
- [2] D.C. Tsui, H.L. Störmer and A.C. Gossard, Phys. Rev. Lett. **48**, 1599 (1982).
- [3] J.M. Leinaas and J. Myrheim, Nuovo Cimento B37, 1 (1977).
- [4] R.B. Laughlin, Phys. Rev. Lett. **50**, 1395 (1983).
- [5] J.K. Jain, Phys. Rev. Lett. **63**, 199 (1989).
- [6] E.J. Bergholtz and A. Karlhede, Phys. Rev. Lett. **94**, 026802 (2005).
- [7] E.J. Bergholtz and A. Karlhede, J. Stat. Mech. (2006) L04001.
- [8] G. Moore and N. Read, Nucl. Phys. B **360**, 362 (1991).
- [9] F.D.M. Haldane, J. Phys. C **101**, 2585 (1981).
- [10] N.K. Wilkin, J.M.F. Gunn, and R.A. Smith, Phys. Rev. Lett. **80**, 2265 (1998).
- [11] N.R. Cooper and N.K. Wilkin, Phys Rev. B **60**, 16279(R) (1999).
- [12] B. Paredes, F. Fedichev, J.I. Cirac, and P. Zoller, Phys. Rev. Lett. **87**, 010402 (2001).
- [13] E.J. Bergholtz, J. Kailasvuori, E. Wikberg, T.H. Hansson and A. Karlhede, Phys. Rev. B **74**, 081308(R) (2006).
- [14] E. Wikberg, E.J. Bergholtz, and A. Karlhede, Preprint, [arXiv:0903.4093].
- [15] E. Ardonne, E.J. Bergholtz, J. Kailasvuori, and E. Wikberg, J. Stat. Mech. (2008) P04016 [arXiv:0802.0675].

- [16] E.H. Hall, Journal of Mathematics **2**, 287 (1879).
- [17] S.M. Girvin, cond-mat/9907002, (1999).
- [18] R.L. Willett, J.P. Eisenstein, H.L. Störmer, D.C. Tsui, A.C. Gossard and J.H. English, Phys. Rev. Lett. **59**, 1776 (1987).
- [19] L.D. Landau and E.M. Lifshitz, *Quantum Mechanics* (Pergamon Press, New York, 1994).
- [20] R.B. Laughlin, Phys. Rev. B **23**, 5632 (1981).
- [21] F.D.M. Haldane, Phys. Rev. Lett. **51**, 605 (1983).
- [22] B.I. Halperin, Phys. Rev. Lett. **52**, 1583, 2390(E) (1984).
- [23] J.K. Jain, Phys. Rev. B **41**, 7653 (1990).
- [24] J.K. Jain, *Composite fermions*, (Cambridge University Press, 2007).
- [25] M. I. Dyakonov, cond-mat/0209206, (2002).
- [26] F. E. Camino, Wei Zhou, V. J. Goldman, Phys. Rev. Lett. **95**, 246802 (2005).
- [27] See e.g. M. H. Freedman, A. Kitaev, M. Larsen and Z. Wang, Bull MAS **40**, 31 (2003); A. Kitaev, Ann. Phys. **303**, 2 (2003). C. Nayak S. H. Simon, A. Stern, M. Freedman, S. Das Sarma, Rev. Mod. Phys. **80**, 1083 (2008).
- [28] F. D. M. Haldane, Phys. Rev. Lett. **55**, 20 (1985).
- [29] D. Yoshioka, B.I. Halperin and P.A. Lee, Phys. Rev. Lett. **50**, 1219 (1983).
- [30] R. Tao, and D.J. Thouless, Phys. Rev. B **28**, 1142 (1983).
- [31] P.W. Anderson, Phys. Rev. B **28**, 2264 (1983).
- [32] W.P. Su, Phys. Rev. B **30**, 1069 (1984).
- [33] W.P. Su and J.R. Schrieffer, Phys. Rev. Lett. **46**, 738 (1981).
- [34] E.J. Bergholtz, T. H. Hansson, M. Hermanns, and A. Karlhede, Phys. Rev. Lett. **99**, 256803 (2007).
- [35] E.J. Bergholtz, and A. Karlhede, Phys. Rev. B **77**, 155308 (2008).

- [36] E.H. Rezayi and N.Read, Phys. Rev. Lett. **72**, 900 (1994).
- [37] B.I. Halperin, P.A. Lee and N. Read, Phys. Rev. B **47**, 7312 (1993).
- [38] E.H. Rezayi and F.D.M. Haldane, Phys. Rev. B **50**, 17199 (1994).
- [39] A. Seidel, H. Fu, D.-H. Lee, J.M. Leinaas and J. Moore, Phys. Rev. Lett. **95**, 266405 (2005).
- [40] M. Greiter, X.-G. Wen and F. Wilczek, Phys. Rev. Lett. **66**, 3205 (1991); Nucl. Phys. **B374**, 567 (1992).
- [41] E.H. Rezayi and F. D. M. Haldane, Phys. Rev. Lett. **84**, 20 (2000).
- [42] F.D.M. Haldane in *The Quantum Hall Effect*, eds. R.E. Prange and S.M. Girvin, (Springer-Verlag, New York, 1990).
- [43] S.A. Trugman and S. Kivelson, Phys. Rev. B **31**, 5280 (1985).
- [44] V.L. Pokrovsky and A.L. Talapov, J. Phys. C **18**, L691 (1985).
- [45] S. Viefers J. Phys.: Condens. Matter **20** 123202 (2008).
- [46] N.R. Cooper, N.K. Wilkin, and J.M.F. Gunn, Phys. Rev. Lett. **87**, 120405 (2001).
- [47] N. Regnault and Th. Jolicoeur, Phys. Rev. Lett. **91**, 030402 (2003); Phys. Rev. B **69**, 235309 (2004); arxiv:cond-mat/0601550 (2006).
- [48] C.C. Chang, N. Regnault, T. Jolicoeur, and J.K. Jain, Phys. Rev. A **72**, 013611 (2005); N. Regnault, C.C. Chang, T. Jolicoeur, and J.K. Jain, J. Phys. B **39**, 89 (2006).
- [49] N. Read, and E.H. Rezayi, Phys. Rev. B **59**, 8084 (1999).
- [50] A. Seidel, and D.-H. Lee, Phys. Rev. Lett. **97**, 056804 (2006).
- [51] N. Read, Phys. Rev. B **73**, 245334 (2006).
- [52] A.Seidel, and K. Yang, Phys. Rev. Lett. **101**, 036804 (2008).
- [53] E. Ardonne, arXiv:0809.0389 (2008).
- [54] F.D.M. Haldane, talk at the 2006 APS March meeting, unpublished.
- [55] B.A. Bernevig, and F.D.M. Haldane, Phys. Rev. Lett. **100**, 246802 (2008); Phys. Rev. B **77**,184502 (2008).

- [56] X.-G. Wen and Z. Wang, Phys. Rev. B. **77**, 235108 (2008); Phys. Rev. B. **78**, 155109 (2008); M Barkeshli and X.-G. Wen, arXiv:0807.2789 (2008).
- [57] S. Jansen, E. H. Lieb and R. Seiler, phys. stat. sol. (b) 245, 439 - 446 (2008); Commun. Math. Phys. **285**, 503 (2009).